האוניברסיטה העברית בירושלים
THE HEBREW UNIVERSITY OF JERUSALEM

THE ROBERT H. SMITH FACULTY OF AGRICULTURE, FOOD AND ENVIRONMENT

Characterizing effluent particles from in-line filtration system

M.Sc. thesis

Department of Soil & Water Sciences
Faculty of Agriculture, Food and Environmental Sciences, Hebrew University

From

Claudio Kohn

Rehovot, Israel 2009

Dedicated to my daughter

This work was done by the advice of:

- Doctor Hadas Mamane, School of Mechanical Engineering, Faculty of Engineering Tel Aviv University

- Professor Avner Adin, Department of Soil & Water Sciences Faculty of Agriculture, Food and Environmental Sciences, Hebrew University of Jerusalem

Acknowledgments and thanks

I must start by thanking my thesis mentors Dr. Hadas Mamane and Prof. Avner Adin for their guidance and support.

I wish to express my deep appreciation to Nelly Izikson and Tomer Krizer for the support in research that was done on Mekorot waste water treatment plant at Shafdan.

Many people provided guidance and advice during my research. There for I am very greatfull to Luba Rubinstein, Rivka Calvo, Haim Zikorel, Jorge Alessandri, Nir Kinory and Roberto Gurovich.

I want to thank my loving family, my parents Polly and Eddy, my brother Andy, for their support and care. I am deeply thankful for their belief and trust, which gave me a power to go on even when it was hard. Without their patience and help I would not be where I am today.

Especially thank to my wife Nadia for her help, love and patience.

This work was partially supported by SWITCH Project

Summary

Israel is situated in a semi-arid zone with insufficient water sources, thus wastewater effluent reuse for irrigation provides a major alternative for fresh water shortage. The search for new treatment technologies and optimization of the current processes are important as an alternative to existing technologies for the whole area. Due to economical needs , the Israeli national water company, Mekorot, initiated a series of research projects to produce and optimize tertiary effluents for unrestricted irrigation. Filtration is used world wide as a tertiary treatment to reduce the concentration of particles, especially because the particles in the effluent can clog drip irrigation systems and enhance membrane fouling.

The relationship between particle shape and size on process removal efficiency has not been widely investigated in wastewater treatment plants (WWTP) and this type of analysis may provide a new look into particles. The objective of this thesis is to determine the relationship between particle shape and size on process removal efficiency.

Bed filtration has been in use throughout the world for at least 40 years. The filtration mechanics have been studied in great depth. Many models have been developed for describing the performance of bed filtration. The removal of particles by bed filtration is complex and depends on multiple parameters such as the chemical and physical characteristics of the water and the suspension. The popular model that is in use today is the tri-stage model where particle removal occurs at the depth of the filter, by transport, diffusion and sedimentation.

Generally the shape of particles in wastewater is very complex as natural particles are not spherical when observing the three-dimensional (3D) images of particles and there are many ways to determine particle size and shape, based on various techniques. There is not a universal way that is applicable to the entire particulate size range and shape. The way to evaluate particle sizing depends on many parameters such as the nature of the suspension or the size of the particles. Comparison of particle sizing

obtained by different methods is difficult. Moreover, particle shape can affect equivalent circle diameter (ECD) and size. It is very difficult to find the connection between the shape of the particle and ECD.

In this study, particle analysis was performed by automated image analysis. The capability to analyze accurately and characterize particle shape and size by image analysis can significantly improve many process units. The use of image analysis is increasingly being recognized as a reliable technique to characterize particle shape, size and distribution. This technology generates data by capturing direct images of each particle in flowing liquids through automated sample introduction, image acquisition and analysis.

One of the most important characteristics of particles in filtration is the circularity. The circularity is a dimensionless number between 0 and 1, where the circularity of 1 represents spherical particles and 0 represents non-spherical particles. Circularity in bed filtration can give significant information as particles with low circularity may deviate from the stream line due to their shape; thus these particles can be caught by a collector. In the media, it means that the particles have a greater chance of spin thus leaving the streamline and coming closer to the collector at the media. For particles with high circularity, it is seen that the efficiency of the filter is lower and the particles pass through the filter. For small particles and larger particles, it is shown that not only is there a detachment process but another process not covered by the literature review. This can be called the streamline process; where particles with the greatest circularity can pass through the media inside the streamline without being collected by the media.

Image analysis can provide information on microorganisms and flocs. This information can be used to analyze parameters of microorganisms, how they attach to organic matter and if the specific microorganisms would like to be near flocs to consume the organic material that is at the flocs or in the water.

Table of content

List of Tables

List of Figures

List of Symbols and Abbreviations

ECD –equivalent circle diameter

CE- converted equivalent

WWTP-wastewater treatment plant

NTU-nephelometric turbidity unit

3D-three dimensional

2D-two dimensional

SEM-Scanning electron Microscope

VDW-Van der Waals

PAC –Poly aluminum Chloride

NPAC-Non Poly aluminum Chloride

UV –Ultra violet

HMP-Hexametaphosphate

TS-total solid

TSS-total suspended solid

MFI-Micro flow imaging

LED –light emitting diode

PSD –Particles size distribution

MFI-Micro Flow Imaging

RRE- relative Removal efficiency

DLVO- theory by Derjaguin and Landau, and Verwey and Overbeek .

1. Introduction

1.1. General

Israel is situated in a semi-arid zone with insufficient water sources, thus wastewater effluent reuse for irrigation provides a major alternative for fresh water shortage. The Israeli national water company, Mekorot, has initiated a series of research projects for producing tertiary effluents for unrestricted irrigation (Aharoni and Cikurel, 2006). One of the projects includes optimization of UV and chlorine disinfection for flocculated filtered effluents. Previous studies showed that particles and wastewater flocs interfere with chemical and physical disinfection (Parker and Darby, 1995; Stewart and Olson, 1996; Emerick et al., 2000; Mamane and Linden, 2006). However these studies did not directly investigate the impact of particle shape on filtration and disinfection efficacy.

Filtration is an advanced tertiary wastewater treatment used to reduce the particulate content of effluents. It is especially important to remove particles from effluents as particles can clog drip irrigation systems and enhance membrane fouling (Adin and Sacks, 1991). Particles in the effluent are generally evaluated through analysis of turbidity. Turbidity is the most common parameter used for monitoring particles however it is insensitive to particles in the size of a few microns (Gregory, 1998), and does not provide information on the size, and concentration of the individual particles in the water. Moreover, turbidity may not be the best true measure of particle removal processes. Adin (Adin, 1999) concluded that optimum removal of submicron particles upon alum coagulation was represented by turbidity measurement while removal of particles larger than 1 μm was measurable best through particle size analyzers. Thus, to obtain more sensitive data on particles it is necessary to employ particle counting methods that provide information on particle size distribution.

The size of irregular particles may be simplified to one parameter by defining particles as spheres and isolating the "equivalent circle diameter" (ECD). Natural particles actually acquire a variety of complex shapes as spheres, ellipsoids, rods, plates or combination of these. Therefore the assumption of particles as spheres is not

satisfactory with particles from water and wastewater effluents as they are not spherical in nature and are frequently in aggregates.

1.2. Objectives

Over the last decades, depth filtration has been studied extensively with respect to particle removal; however removal was usually based on size and not on other parameters such as shape. Knowledge of the number, size and shape distribution of the particles present in water, before and after filtration, can provide designers and operators means for improving filtration efficiency. Although the shape has been stated as significant for various processes, the relationship between particle shape and size on process removal efficiency has not been widely investigated in wastewater treatment plants (WWTP) and this type of analysis may provide a new look into particles. The objective of this thesis is to determine the relationship between particle shape and size on process removal efficiency.

2. Literature review

2.1. Particle removal mechanisms in granular filtration

Bed filtration has been in use throughout the world for at least 40 years. The filtration mechanics have been studied in great depth. Many models have been developed for the performance of the bed filtration .The removal of particles by bed filtration is complex and depends on multiple parameters such as the chemical and physical characteristics of the water and the suspension. Particle removal mechanisms are discussed and reviewed in this section. The popular model that is in use today is the tri-stage model where particle removal occurs at the depth of the filter. The basis of the process was defined by O'Melia and Strumm in 1967. They determined that the process occurs in two steps, the transport step and the attachment step. However Minst et al., (1967) proposed a third step, the detachment mechanism, which is detailed in section 2.1.5.

2.1.1 The Transport step

The transport step is the step when particles came close to the collector at the media and occurs by interception of the particles with the collector, diffusion to the collector, and by sedimentation of the particles. The transport step proposed by of O'Melia and Strumm (1967) is the step where the physical hydraulic forces the mass to move. Ives (1973) showed that the transport step is the step that makes the particles move from the line flow and permits them to strike an absorbing grain. Darby et al., (1992) proposed that the efficiency of transport depends on the number of times particles strike the grains versus those that only come near to the grains at the end. A detailed summary of the transport step is presented by Amirtharajah et al., (1988).

2.1.2 Interception

A strike incident occurs when the line flow moves near the grain and the particles can attach to the grain in the media.

2.1.3 Diffusion

Diffusion occurs due to Brownian motion of particles. This movement can cause the particles to move from the line flow. This mechanism occurs only to particles not larger than 1 μm.

2.1.4 Sedimentation

This mechanism uses gravitational force and depends on the velocity and size of the particle. If the density of the particle is greater than the transport liquid, this can cause the particles to move from the line flow with the gravitational force. The mechanism of sedimentation shows that the efficiency of the process depends on the temperature of the liquid and the density of the particles and is appropriate for particles of 5–25 μm (Yao et al., 1971) .This mechanism is the important mechanism for the removal of the parasite Giardia *Lamblia* in the size of 10–15 microns, which have been filtered by straining (Tufenkji et al. 2004). Another mechanism is where the particles can rotate and start spinning. This depends on their shape. Longer particles can rotate and easily leave a flow line. The inner mechanics have not been investigated at depth because of the difficulties of particle shape calculation.

Figure 2.1 illustrates log removal versus particle diameter. A minimum removal is observed at approximately 3 micron diameter. This phenomenon is called the minimum transport mechanism because particles of this diameters pass throw the media. Particles such as *Cryptosporidium Parvum*, a protozoa that causes intestinal diseases, at size of 3–5 microns, is found at minimum transport, therefore does not attach to the collector and consequently can be barely filtrated (Adin and Elimelech, 1989).

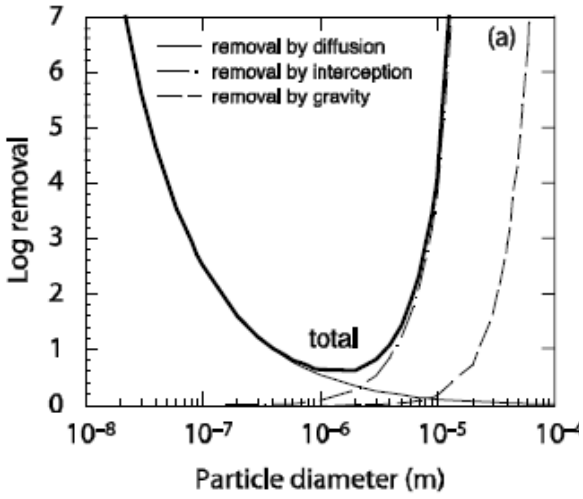

Figure 2.1: Log removal versus particle diameter (Adin and Elimelech, 1989)

2.1.5 Detachment mechanics

The detachment mechanism conflict took a long time to resolve. Minst, (1967) claimed that the sedimentation of particles at the media causes the velocity of flow to increase and particles detach from the media. Ives (1969) stated that the detachment process is not important and the sedimentation of particles at the filter causes the velocity at the media to increase to a level that makes filtration impossible.

2.1.6 Ripening step

There is a consensus by researchers that at the beginning of a filtration process efficiency of the filter is low and particles that have been collected in the media of the filter improve the filter's efficiency by functioning as a new collector of particles (Darby et al. 1992). Darby et al. (1992) concluded that the ripening process is characterized by a winding,

where the filter starts to remove the particles more efficiently. This point refers to the area of the media and the addition of particles improves filtration efficiency. Improvement of the filtration efficiency makes up for the head loss on the filter (Darby et al., 1991). Adin and Rebhun (1974) described bed filtration process where the filtration process does not occur at the upper layer of the filter and occurs inside the filter. The filter works until the filter is saturated because the accumulation of particles. The next filter layer then starts working. This model is similar to the absorption models. The ripening step depends on the type of coagulant used. Adin and Rebhun (1974) found a correlation between the time of ripening and the type of coagulant. Between alum and polymer, they found that the alum ripening time is less than that of the polymer.

2.1.7 Filtration optimization

There are two parameters that are significant in determining the efficiency of the filter:

Quality of the outflow - The quality of the outflow must be in correlation to the regulation or use of the outflow. It is not effective to have an outflow with 0.2 NTU turbidity when regulations require, for example, at least 1 NTU.

Filtration time - The backwash step takes time, energy and amortization of the system. The longer the filtration time, the more efficient is the filter. Mintz, (1966) concluded that the time t_1 is the time needed for a poor quality outflow, while t_2 is the time that head loss reaches the highest values. The filtration time is the best when $t_1 = t_2$.

t_1 = time that take the filter to get poor water quality of filtration outflow;

t_2 =time that take the filter to get high head loss

2.2. Particle counting

2.2.1. Particle size

Generally the shape of particles in the wastewater is very complex as natural particles are not spherical when observing the three-dimensional (3D) images of particles. The equivalent diameter of particles is a significant parameter used to describe particle size or shape. Of course differently shaped particles will have an influence on this Equivalent Circle Diameter (ECD), but, more importantly, it is a single number that is larger or smaller as the particle size becomes larger or smaller and is objective and repeatable. The 3D image of the particle is captured as a two-dimensional (2D) image and converted to a circle of equivalent area to the 2D image. Figure 2.2 shows a computer analysis of the particles. The diameter of a circle is then reported as the converted equivalent (CE) diameter (Malvern website, 2005).

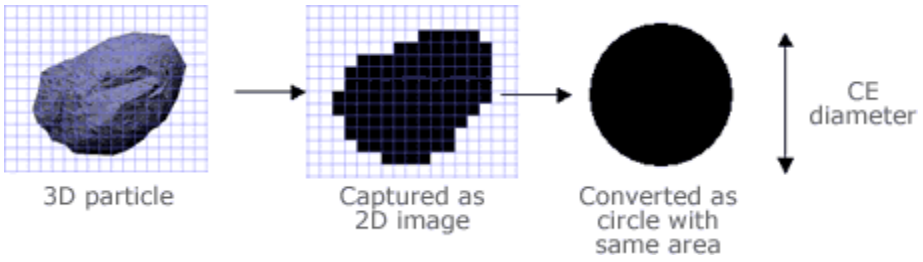

Figure 2.2: Conversion of particle captured image to CE diameter

An appropriate single characterization number would be the mean of all the equivalent circular diameters.

2.2.2. Measurement of particle size and shape

There are many ways to determine particle size and shape, based on various techniques, but there is not a universal way that is applicable to the entire size range and shape. The way to evaluate particle sizing depends on many parameters such as the nature of the suspension or the size of the particles. Comparison of particle sizing obtained by different methods is difficult. Moreover, particle shape can affect ECD and size. It is very difficult

to find the connection between the shape of the particle and ECD. Different technologies are used to measure particle size and shape as follows:

2.2.3. Microscopy

Optical microscopy is limited by the wavelength of visible light, so particles that are smaller than 1 micron are difficult to resolve. In fact, particles sizes smaller than 5 microns are difficult to derive. Particles in wastewater can be enumerated microscopically by counting individual particles and stains can be added to aid in differentiation. However analysis of particles by microscopy is limited to a small number of images thus data is not statistically representative, data analysis is laborious and results can be subjective. The size shape of particles as observed by Scanning Electron Microscopy (SEM) may be correlated to the processes wastewater effluents undergo and may correspond to different origins of the wastes, as reflected via the distribution of elements in different flocs and detected by SEM-EDX (energy-dispersive X-ray spectroscopy) analysis (Adin at al., 1989). The Confocal Laser Scanning Microscope, in which a small sample of suspension is illuminated by a laser beam, the laser scans the particle layer in the way a 3D image can be built and provides a much higher resolution than a conventional light microscope.

2.2.4. Coulter Counter

This is a common method for counting the number of particles and for determining the concentration of each particle. It was originally developed for sizing blood cells. An electrical signal proportional to the volume of the particle is produced as particles are swept through the orifice by a flow of the electrolyte. This method uses an electric circuit formed between the two electrodes, anode and cathode, immersed in an electrolyte on the opposite side of the small orifice. Due to the flow of electrolyte, the particle swept through the orifice results in the production of an electric signal proportional to the volume of the particle. This electrical signal is converted into a measurable value.

2.2.5 Image analysis

In this project, particle analysis will be performed by image analysis. The capability to analyze accurately and characterize particle shape and size by image analysis can significantly improve many process units. The use of image analysis is increasingly being recognized as the most reliable technique to characterize particle shape and characterize a particle size and volume distribution. This technology generates data by capturing direct images of each particle in flowing liquids through automated sample introduction, image acquisition and analysis. Particle shape analysis has become a critical parameter in many industrial processes. This has fueled a demand for increasingly flexible analytical systems that can be used in a variety of different circumstances to provide shape and size information quickly and easily.

2.2.6 Geometric characteristics

Digital characteristic of the picture is taken at each frame. These characteristics are expressed in the following parameters:

ECD - The measurement is done by counting the pixels that represent the magnified image of the particles. This translates the area of the pixels in μm and uses an algorithm that calculates the ECD of the particles. The 3D picture converts to a 2D picture, counts the pixels, and converts to a circle. Equation 2.1 allows calculating the ECD by the use of the area of the particle.

$$ECD(\mu m) = 2 \cdot \sqrt{\frac{a}{\pi}} \qquad (2.1)$$

$$a = area,\ \mu m^2$$

Feret - Max Feret is the maximum diameter between two points on the perimeter between which a line can be drawn within the perimeter. The picture is rotated and the imaging analysis system measures the length between two points and finds the longest length between two points as it show at figure 2.3.

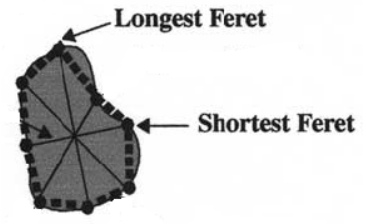

Figure 2.3: Feret definition

Area - the area is the total number of pixels covering the object area.

Circularity - The circularity is a dimensionless number between 0 and 1, where the circularity of 1 represents spherical particles and 0 no spherical particles. It defined as an equivalent circle divided by the perimeter of the particle as is show in Figure 2.4.

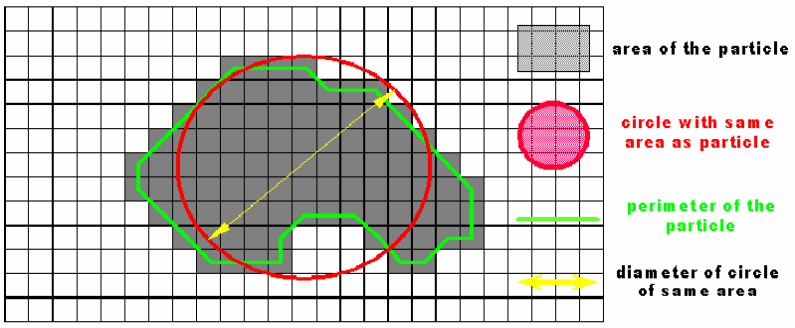

Figure 2.4: Calculation of circularity

Intensity - Intensity represents the photocurrent generated by the pixels in the digital camera's sensor array. The photocurrent intensity values range from 1 to 1024, where 1024 is brightest (white) and 1 represents darkest (black). Threshold is the process by which the system differentiates between a darker pixel that represents a particle, versus a

brighter pixel that represents the carried fluid. This is critical to the process in the imagining analysis to determine what the particle and the fluid are.

2.2.7 Limitations of the image analysis process

There are some issues to consider in calculation and estimation if the processes used to obtain genuine result that are truly representative of the particles examined. Most of the parameters are received by the pixel thus the resolution of the pixel can be a significant parameter. If the resolution is higher, each pixel will be smaller. Figure 2.5 shows that particles of 10 μm diameter have an area of 78 $\mu m^2$and if each pixel has a length of 2 μm, the area of the particle will be 25 pixels. However, if each pixel has a length of 0.25 μm, the same particle will be 1600 pixels and the resolution of the picture will be greater and more accurate. This process can be improved by using lenses and magnification that increase pixel resolution.

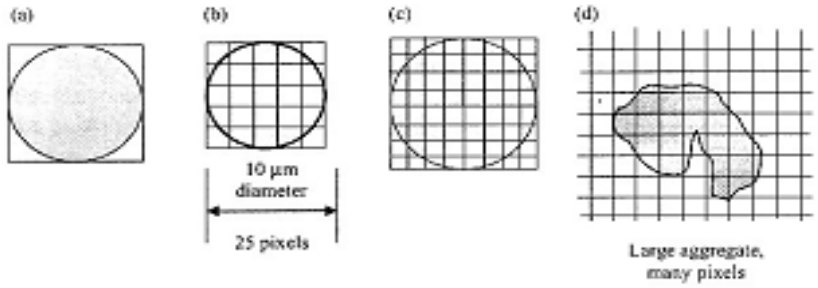

Figure 2.5: Pixel resolution

2.3 Fractal dimension of aggregates by image analysis

The fractal dimension, a parameter emerging from the Fractal Theory (Li, et al., 1989), is a generic term without a restricted definition that embraces a wide range of different, yet interrelated dimensions (Glasbey et al, 1994). It provides the means to measure the complexity and irregularity of the objects. Aggregates can be recognized as self-similar. With fractal objects this means aggregate or flocs may have a similar shape, independent of size. As shown in Figure 2.6, the particles are similar, but their size and shape are different.

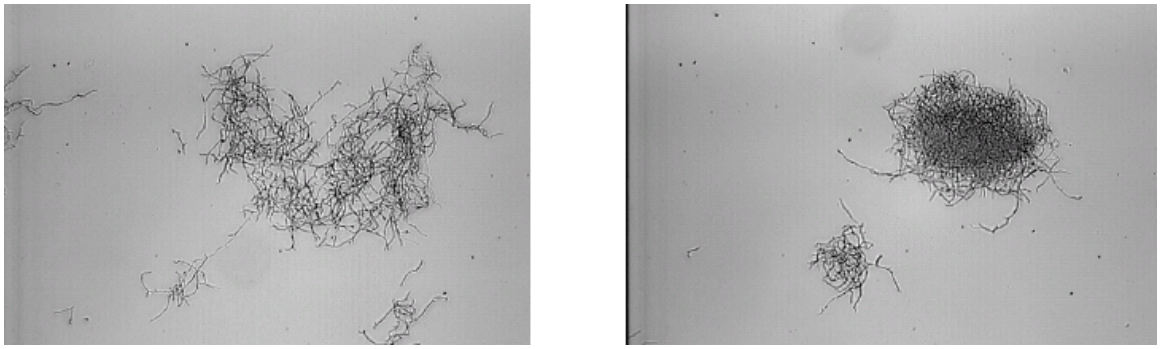

Figure 2.6: Particles in activated sludge.

Aggregates of particles have fractal characteristics such as the mass of the aggregate. The 2D plane is filled uniformly with objects that increase the size of the table and hence the square of a linear measure.

(2.2) $M(R) \alpha R^{D}$

M=mass of a fractal

R=size

d_f = fractal dimensions

Equation 2.2 explains how a log plot of M versus R gives a straight line with a slope of D. In 3D space the fractal dimensions values are between 1.4 to 2.8(Li, et al., 1989), where potential energy diagrams D is a linear aggregate, which is the mass proportional to the length, and for a uniform aggregate, non fractal, the mass should vary as the cube of the size. There are some models that can explain the formation of aggregate by fractal structure. In the beginning the particles arrive as single particles, join together and tend to create compact flocs. When there is floc to floc collision, more open flocs are created (Elimelech, 1995). One of the most important uses of fractal structure of aggregates is

density. The density of the aggregates decreases as size increases. This is important when the solid-liquid separation process occurs, especially when it is a sedimentation process. Image analysis can be useful in investigating fractal dimension, but it is affected by the resolution of the imaging and pixel representation by the picture, if the imaging analysis system is not precise in pixel representation.

2.4 Colloid interaction and colloid stability

Particles in water interact between each other and this interaction can vary depending on their properties such as surface proprieties properties and size of the particles. Many forces interact between the particles and can cause attraction or repulsion between the particles. When particles repel each other and keep apart and are not aggregated, the particles are unstable. This concept is called colloid stability and the interactions are called colloid interaction. This is colloid because this interaction and stability affect the colloidal size particles.

2.4.1 Types of interactions

Van der Waals (VDW) and electrical double layer - this quantitative theory is based on colloid stability developed by Derjaguin and Landau, and Verwey and Overbeek (DLVO) independently in 1940. This theory is known as the DLVO theory (Churaev NV, 1999). The classical DLVO Model of the electrical double layer describe coagulation as a collision between two colloids leading to aggregation depending on the attractive forces (VDW) and the repulsive electrostatic forces that result from the negative electric charge of most colloids (Buffle and Leppard, 1995; Buffle and van Leeuwen, 1993). Sum forces can be either repulsive or attractive depending on media, chemical structure and surface potential. Hydration effect, hydrophobic, steric and absorbed layers and polymer bridging are interactions that are non-DVLO forces.

2.4.2 Potential energy diagrams

The combined interaction of Van der Waals and the electrical double layer are additive. The interaction between particles can be explained as shown in 2.7, and is defined by the energy interaction and the separation distance between two identical spheres. The potential energy diagram is important in order to understand colloid stability. The most

important feature of this diagram is the large potential energy barrier. Particles need to pass this energy barrier to be in contact with each other. Because of this barrier, which is higher from the thermal energy of the particles, it is unlikely that particles will go through this barrier.

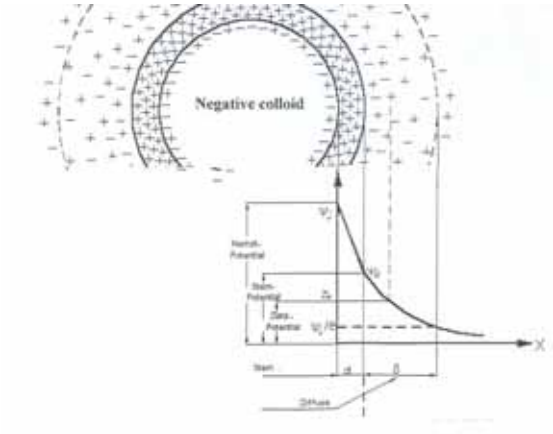

Figure 2.7: potential energy diagram

2.5. Soil separation

Particles may range in size from a few nanometers on the border between dissolved and colloids, sub-micron, micron range and up to millimeter dimension as with sand particles. A distinction is being drawn between colloidal and suspended particles, with an arbitrary boundary of 1 μm or of 0.45 μm defined as boundary to suspended solids measurements in wastewater characterization. Colloidal particles vary between 0.001-1 μm, and dissolved constituents are typically smaller than 0.001 μm, however the distinction may depend on quantification method of colloids and dissolved constituents. For the particles of a small size, such as clay silt, and sand, Stokes' Law is used for separation. Figure 2.8 shows how particles are qualified by size and classified in different systems.

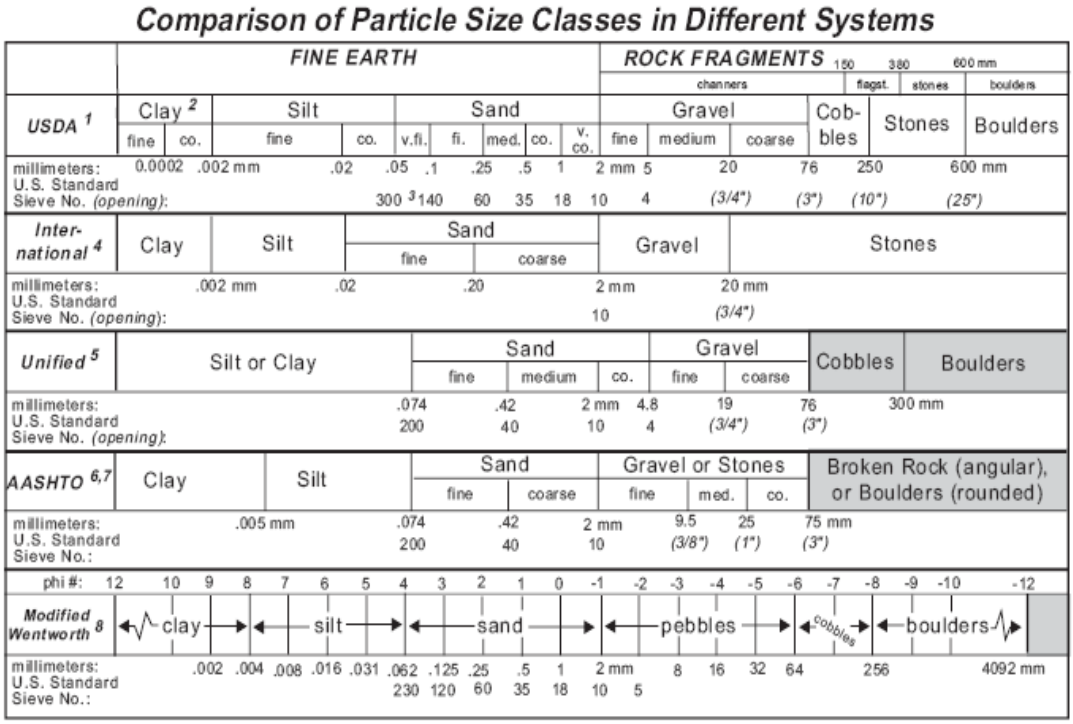

Figure 2.8: Particle size classes

Sedimentation analysis relies on the relationship between settling velocity and particle diameters. Settling velocity is related to the diameter of a spherical particle. This relationship was first developed by Stokes (1851) and it is known as Stokes' Law. Basics used in applying Stokes' Law to sedimentation soil in suspension are:

- Terminal velocity starts as soon as settling begins
- Settling and resistance are due to the viscosity of the fluid
- Particles are smooth and spherical
- There is no interaction between the particles

Since soil particles are not smooth and spherical, the diameter must be equivalent to the actual diameter. The assumptions of Stokes' Law as applied to soil are more fully discussed by Krumbein and Pettijohn (1938).

2.6. Deflocculation

A "dispersant" is an agent that is added to a fluid that makes the colloids and particles to disperse from each other. The deflocculants are added to the fluid to make the particles separate from each other. For example anionic molecules can neutralize the charge of particles such as clay, destabilize the structure and make the clay particles to separate. The use of deflocculant in research of particles characterization is important and more important is the decision of which deflocculant to use because the separation between the particles is mechanical and if the separation is to much aggressive it can affect the characteristics of the particles by changing the size and especially to the shape.

2.7 Conclusions from the Literature Review

The research of particles and filtration have been investigated for a long time and the theory of particles behavior has a solid basis, but the natural particles behavior in water and especially in wastewater treatment have not been researched deeply. It is difficult to understand and analyze particles in water as the concentration of the particles in waste water is high, it is difficult to obtain statistical data, the standard deviation is high and there are different types of shapes of particles in the same type of water.

There are many ways to determine particle size and shape, based on various techniques, but there is not a universal way that is applicable to the entire size range and shape. The way to evaluate particle sizing depends on many parameters such as the nature of the suspension or the size of the particles.

There are many types of technologies that based on investigation of particles in water. Turbidity does not give information on the concentration and the shape of particles in water, but gives a good and simple information of the quality of water and this is the reason of the big use worldwide. Other technologies, like particles size distribution, give good information on the concentration of the particles, but do not give shape parameters.

Confocal Laser Scanning Microscope that can provide 3D particles view but does not give concentration of particles in water.

Image analysis can be useful for investigation of the behavior of particles in wastewater filtration. Statistical data of the concentration and 2D shape of particles can be obtained as thousands of particles per milliliter can be analyzed. There is a possibility to determine different types of particles by observing the image and to finding the difference between inorganic particles, activated sludge flocs and microorganisms.

At can be studied from the literature review, it is obvious that the research of particles in the wastewater is not completed and new research topics should be explored.

3 Experimental methods and materials

3.1. Pilot plant

3.1.1 Pilot plant description

The pilot is designed to produce tertiary treated effluents for unrestricted irrigation (Halperin Committee Guidelines, 1999) and it is located in the Dan region wastewater treatment plant (WWTP) in Shafdan. The pilot plant consists of a system with a bed filtration and disinfection system. Pilot system operation will allow decision makers to evaluate the economic worth, location, need, quality, and additional parameters of a full scale system. Results from the pilot plant will also provide answers to the preliminary requirements. Based on the information gathered from pilot plant operation, a fully-functional system can be constructed.

The secondary effluent flows into the tertiary treatment. This treatment is based on a direct filtration process that integrates coagulants during the process. The effluent enters from a 400 micron automatic filter in order to remove large objects that can block the bed filter, the water continues upward into the two sand filters which keep the media filter straight with a flow of 3.2 m^3/hr each with a velocity of 12 m/hr. A control system is responsible for measurement of the pressure before and after the filter that automatically controls the backwash. The filtration process runs for 6 to 8 hours or 3 meters of head loss and depends on the quality of water, coagulant applied, flow velocity, and temperature of the water.

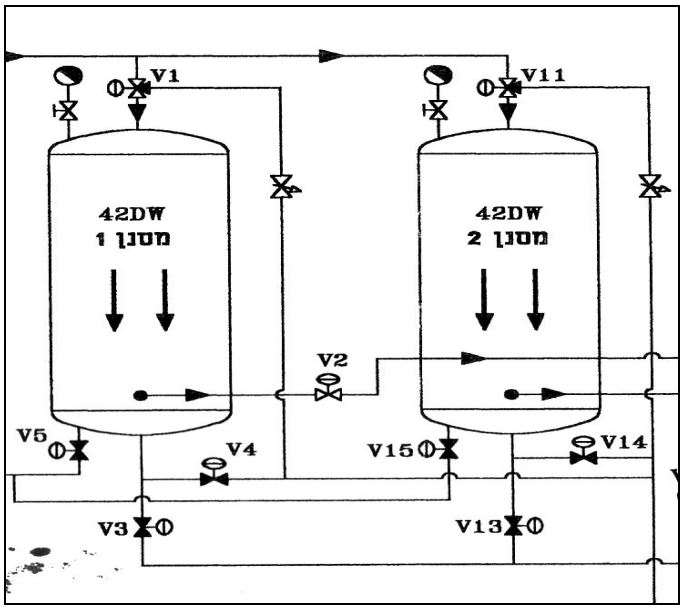

Figure 3.1: Schematic of sand filtration system

The system can work in parallel, where the water passes through both filters or in sequence, when where water flows through only one filter after the other. All presented tests were done when the system worked in parallel mode.

Figure 3. shows how the filter can work in parallel or in sequence by only changing valves V1, V11, V4, and V14.

3.1.2. Equipment

Inlet pump - Centrifugal pump with a frequency controller that controls the flow through the filter.

Backwash pump - Centrifugal pump that takes and cleans water and cleans the media in the filter.

Dosing pump number 1 - diaphragm pump that injects the coagulant to the filter.

Dosing pump number 2 - diaphragm pump that injects the chlorine to the cleaning tank.

Dosing pump number 3 - diaphragm pump that injects the chlorine to the filter when is in backwash step

Blower - air blower that puts air into the filter when the filter is in cleaning mode.

3.1.3. Filtration process

Before the water enters the filter there is an injection of flocculants on the media filter that creates contact flocculation. The concentration is 1–3 mg/liter of poly aluminum chloride (PAC). After backwash, a ripening period is taken into account. The ripening period generally lasts from 15 minutes to 1 hour after the backwash event is completed. The end of filter ripening is defined when a significant change in the filtrate turbidity reduction rate occurs, after which filtrate turbidity returns to normal filtration values and the filtration process continues until the backwash process starts again.

Stage	Time (sec)
Backwash	60
Drain	180
Air wash	180
Backwash	180
Direct wash	120

Table 3.1: Sequence of filtration

3.1.4. The backwash stage

At the backwash steps, the backwash flow is important because if the velocity is too high to the bed, the media can escape from the filter. Flow is 11 meter^3/hr. Chlorine is injected into the backwash water to kill microorganisms that are in the bed after the filtration. The concentration is at 10 mg/liter. The control system controls all the parameters of the pilot plant online and can work alone without any human intervention: flow-in filter, turbidity, pressure before and after the filter, backwash control, and temperature.

3.1.5. Filter parameters

The table below represents general parameters of the system.

Table 3.2. Filter parameters in Shafdan pilot plant

Process	**Function**
Type of filtration	Deep bed high rate
Water supply source	Secondary effluents 20/30
Filter height	1.4 meter
Filter diameter	0.6096 meter
Flocculants	Addition of 1–3 mg/l PAC flocculant
Number of filters	2 parallel
Depth of base media	0.01 meter
Anthracite depth	0.6 meter
Sand depth	0.3 meter
Size of base media	(2.5-5) mm
Size of anthracite media	(0.6-0.8) mm
Size of granular media	(1.2-1.4) mm
Anthracite/sand uniformity coefficients	(1.4–1.5)/1.2
Anthracite/sand effective size	(1.8–2.2)/(0.6–0.8) mm
Size of particles	2 mm
Filter water turbidity level before filtration	2.5–5 NTU
Filter water turbidity level after direct filtration	(0.5–0.6) NTU
Filter backwash flow rate	11 (m^3/hour)
Backwash tank volume	10 (m^3)
Filtration rate	15 (m/sec)
Max pressure allowed during run	(200–800) kpa

Chlorination conc. during wash	10 (mg/liter)

3.2. Sample type

The goal is to determine filter removal efficiency through particle size and shape parameters. Different types of wastewater samples were used for comparison of the different parameters of the particles as follows:

1. PAC and NPAC particles: The coagulant Poly Aluminum Chloride (PAC) at concentration of 2-2.5 mg/L was added directly on the filter media to improve filtration in a process termed in-line filtration while the other filter is identical but without addition of coagulant. Samples for analysis include secondary effluent prior to filtration and samples after filtration. Samples after filtration will be termed "PAC" or "NPAC" for filtration with or without PAC respectively.

2. Backwash samples: water after backwash was collected for analysis.
3. Secondary Effluent after UV and Chlorine Disinfection and Photo-Reactivation with Solar Radiation: additional samples after secondary treatment in another WWTP (Ramat HaSharon, Israel) after UV or chlorine disinfection are held in a reservoir and examined after two weeks to study the correlation between size and shape parameters and to find how particles, especially microorganisms, behave after photo-reactivation. These samples will be termed "Chlorine" or "UV".
4. Natural Silt Particles: inorganic sample taken from soil and separated to the silt fraction was analyzed and termed "Silt". Soil samples were collected from the North Negev region, Israel which is characterized by high silt content. The separation method for the silt fraction was based on the piped method as detailed in section 3.6.
5. Polystyerne microspheres and latex beads: 5 and 10 μm polystyrene microspheres and 90 μm latex beads. System calibration is conducted with polymer microspheres with mean diameters of 5 μm ± 0.05 μm and 10 μm ± 0.1 μm with narrow size distributions and certified by manufacturer (Duke

scientific, USA). Latex beads at a size of 90.7 ± 17.7 μm. The particles are sonicated and then diluted in deionized water.

3.3. Porosity

Porous materials are solid materials with pores (holes) between each other. Liquid and gas can pass through these pores. Materials that have pores inside of the particles are called permeable porous materials (such as activated carbon). The material used as a bed filter is not a permeable porous material and for the calculation of the retention time at the filter there is a need to calculate the ratio between the pores and the solid material. For the calculation a measuring tube of 100 ml, dry 105°C filter media, and boiled water at 25°C is required. The measuring tube is filled with the dry 105°C filter material at volume of 25 ml (gently tap) and the process is repeated for 35 ml, 45 ml, etc. until 100 ml is reached. The measuring tube is filled with water until it reaches 100 ml and is gently tapped to release all the air from inside. The volume of water inside the measuring tube is measured and porosity is calculated with Equation 3.1 where V_w is the water volume and V_t is the total volume.

$$3.1.\ \phi = \frac{V_w}{V_t}$$

3.4 Turbidity

Turbidity is a measure of light transmitting properties of water, and is one of the most common tests to indicate quality of water and evidence of particles. The measurement of turbidity is based on comparison of the intensity of light scattered by a sample at 90 degrees to the path of incident light to the light scattered by a reference sample. Turbidity in water and wastewater is caused by suspended and colloidal particles as clay, finely divided organic and inorganic matter, and microscopic organisms (APHA, 2005). Turbidity provides information on the colloidal particles (<1 μm) thus can be a measure of colloidal removal. Turbidity is not a direct measure of the particles in water or how the particles scatter the light, but a gives a good measurement of the clarity and quality of the water. The instrument used is a Hach 2100P Portable Turbidimeter with a range of 0–

1000 NTU and accuracy of 0.1 NTU. Selectable signal averaging mode compensates signal averaging for fluctuations in readings caused by movement of large particles in the light path. The turbidimeter was calibrated before each experiment with four sealed vials of StablCal Primary Turbidity Standards (<0.1, 20, 100, and 800 NTU).

3.5. Coagulants

The coagulant is PAC at 18% concentration, 30 kg tanks. The coagulant was diluted to 1.8% and added with a diaphragm dosing pump at concentrations of 2–2.5 mg/liter directly to the top of the media, where the coagulant came in contact with the water before it entered the media. The other filter is the same, but without the addition of a coagulant.

3.6. The piped method

The piped method was adapted by Day (1965) and Green (1981). The piped method is a direct sampling procedure. It depends on taking a small sample by a pipe at a depth using Stokes' Law. Figure 3.2 shows how the system is built to test sedimentation of particles.

Materials used for this method are: Cylinder, 1000 ml, Ruler capable of measuring to 250 mm, Support rod, Vacuum pump, Flexible tubing, Pipette, Sliding clamp, Sodium hexametaphosphate (HMP) solution (5%), Sieves with 2 mm square holes and Mixer. The procedure is as follows:

To calculate the time the following formula is used:

$$t = {}^{18\eta h}\!\!\diagup\!\!\!\diagdown_{\left[g(\rho_s - \rho_1)x^2\right]}$$

$$\rho_1 = \rho^0(1 + 0.630C)$$

$$\eta = \eta^0(1 + 4.24C)$$

$\eta =$ Fluid viscosity at temperature (t)

$\eta^0 =$ Water viscosity at temperature (t)

$h =$ Depth after time t

$g =$ Acceleration due to gravity

$\rho_s =$ Particle density

$\rho_1 =$ Liquid density at temperature (t)

$\rho^0 =$ Water density at temperature (t)

x = Equivalent diameter of soil particles

For determination of the silt fraction: weigh 100 grams of soil, after passing through the 2 mm sieve square holes, add 125 ml of HMP 125 ml, fill to 1 liter and shake with the mixer for a few minutes and introduce the solution to the cylinder, measure the time, and take the sample after this time.

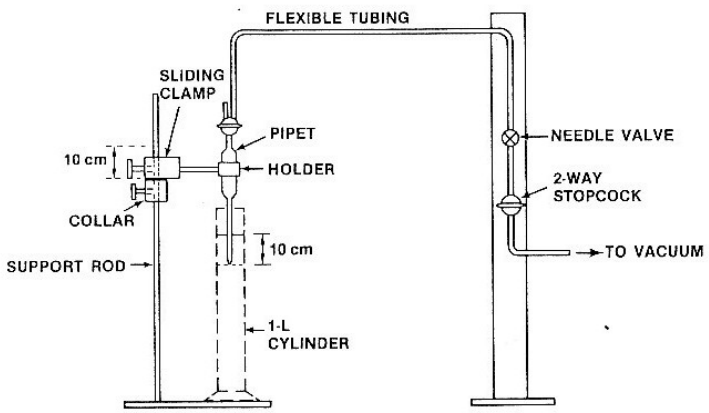

Fig. 15–5. Schematic diagram of pipet stand and apparatus for sedimentation analysis.

Figure 3.2: Schematic diagram of sedimentation analysis

3.7. pH and conductivity

An IQ Q170NP multi-parameter system with non-glass IFSET probe, PHW77-SS pH Probe, and CDW97-KP5 Conductivity Probe were used for the pH and conductivity measurement. The pH meter has automatic and manual temperature compensation and the conductivity cell probe has auto-ranging. The pH meter was calibrated before each experiment with a pH calibration kit with 4.0, 7.0, 10.0 pH buffers. Conductivity was calibrated with solutions of 100 uS, 1000 uS, 10,000 uS.

3.8. Temperature

Temperature was measured with a simple laboratory thermometer with an accuracy of 0.1°C

3.9. Total suspended solids

Total solids (TS) are obtained after evaporating a sample to dryness and measuring mass of the residue. Total suspended solid (TSS) is the portion of TS retained by a filter (usually 0.45 μm but ranging till 2.0 μm) measured after being dried (Metcalf and eddy, 2004). The test is based on Standard Method 2540-D. The sample was filtered through a weighted glass filter and the residue retained on the filter after it was dried at 105°C. The increase in weight of the filter represents the total suspended solids. A GFC filter was used and was ignited at 550°C before use and was in a desiccator. The volume of the sample was chosen to yield between 2.5 and 200 mg of residue. If the filtration lasts more than 10 minutes, there is a decreased sample volume.

Correlation of turbidity with the weight or particle number concentration of suspended matter is difficult because the size, shape, and refractive index of the particles affect the light-scattering properties of the suspension

3.10. Imaging analysis

Particles suspended in liquid are analyzed by the "Micro Flow Imaging" (MFI) technology (DPA 4100, Brightwell Technologies Inc, Ottawa Ontario, Canada; www.brightwelltech.com). This apparatus employs a digital camera with an illumination and magnification system to capture in-situ images of suspended particles in a flowing sample. Figure 3.3 shows the entire system set up.

Figure 3.3: DPA4100 micro-flow imaging (Brightwell Technologies)

3.10.1 Overview techniques of the system.

The DPA4100 is an image analysis instrument using micro-flow imaging that captures images of cells or particles suspended in a flowing fluid. The DPA4100 is an electrical process that uses a light emitting diode (LED) with a nominal peak wavelength of 475 nm. The operation of this technology requires wearing protective eye glasses designed to block harmful radiation (class 2). Micro-flow imaging integrates the capabilities of digital microscopy, micro-flow techniques as image processing into a single instrument for automatic analysis of suspended cells and particles. These images are analyzed, and a database is produced consisting of particle count, size, transparency, perimeter, area, and circularity. The database can be interrogated to produce parameter distributions, scatter plots, and isolated images of particle populations of interest. The sample volume in each frame is precisely defined by the flow cell geometry, resulting in absolute determination of particle concentrations (www.BrightwellTech.com). Figure 3.4 shows how the system takes the pictures. Basically a sample fluid is drawn through a flow cell and a sections of the fluid are illuminated with LED light source at λ= 475 nm, magnified and imaged onto a digital camera. These captures images are automatically analyzed to determine various size and shape parameters that represent the two dimensional projection of the particles.

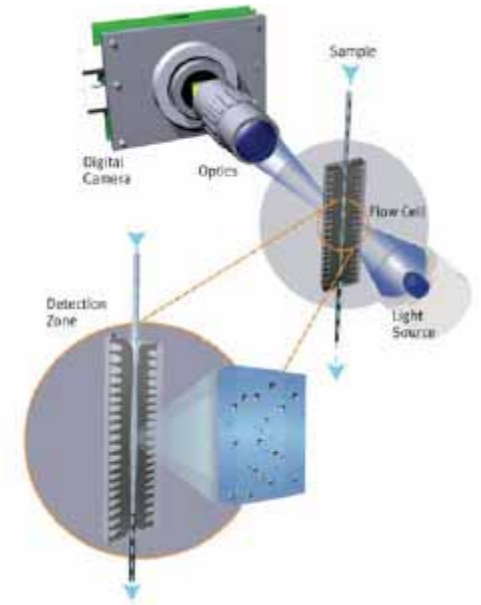

Figure 3.4: imaging process

4. Results and discussion

4.1. Image analysis of microorganisms

Using imaging analysis it is possible to receive information on microorganisms and flocs in water (Clancy and McCuin, 2005; Chakraborti and Atkinson, 2006). This information can be used to analyze parameters of microorganisms, how they attach to organic matter and if the specific microorganisms would like to be near flocs to consume the organic material that is at the flocs or in the water. Microorganism such as the Arcella, a testate (shelled) Amoeba common in activated sludge, epitomizes a type of Protozoa and Rotifers, 100–500 μm long are common in freshwater throughout the world although there are a few saltwater species. Rotifers may be free swimming which creates a current that sweeps food into the mouth, where it is chewed up by a characteristic pharynx containing tiny jaws. It also pulls the animal, when unattached, through the water. Figure 0.1 shows how it can be useful to describe the morphological structure of these microorganisms by image analysis and to know where the microorganisms are located. It can be seen how a Rotifer is located near to a floc to find food. This large floc can protect microorganisms from disinfection by diffusion of chlorine or the photon attack by ultraviolet (UV) disinfection. Rotifers can be easily detected on the image as they are very different than the flocs.

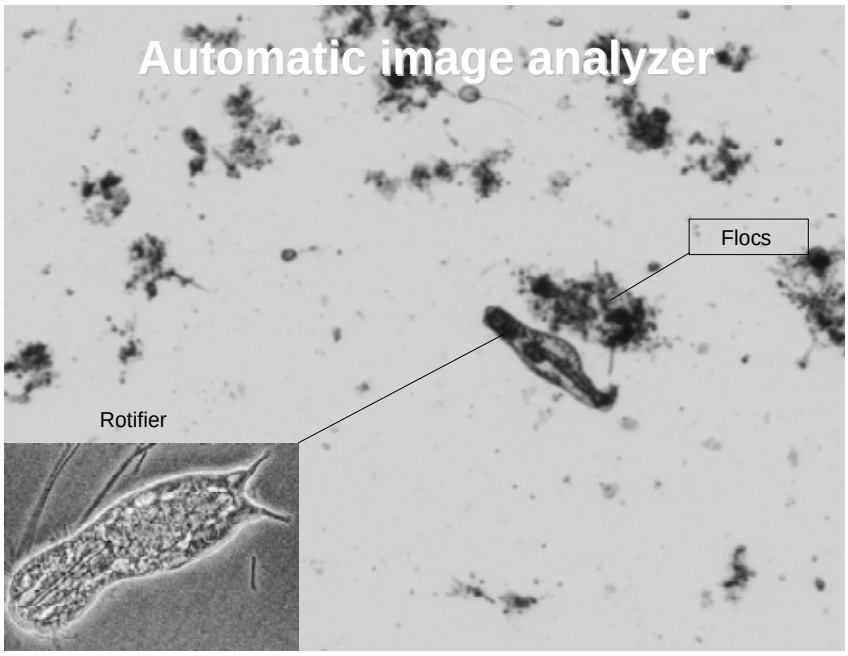

Figure 0.1: Image analysis of rotifers in wastewater sample.

Figure 4.2 and 4.3 show how the system analyzes and process the picture; meaning every point receives a number and the system provides all determined data (size, shape). As it appears in Figure 4.2 and 4.3, upon analysis of the data the system takes the rotifer and floc together. The picture process is erroneous as it is expected to receive the data on the rotifer but the system provides data on the rotifer and floc data together. One particle is obtained instead of obtaining two separate particles when the first is a microorganism and the second is a floc. However it is possible to detect different types of microorganisms from the pictures.

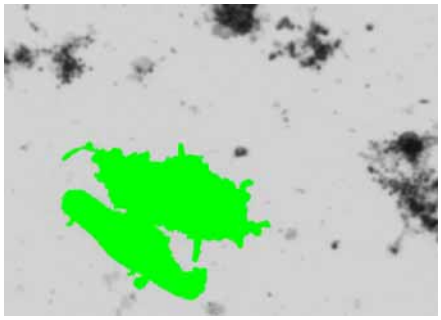

Figure 4.2: Image analysis of rotifers in wastewater sample as used for data analysis

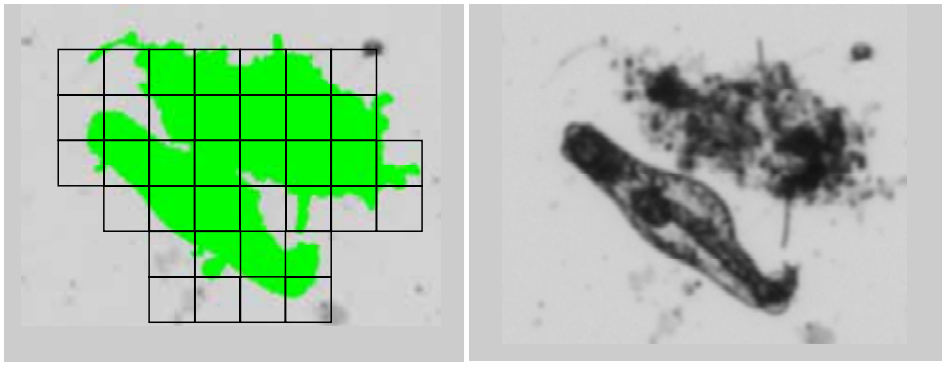

Figure 4.3. Data process of imagining analysis

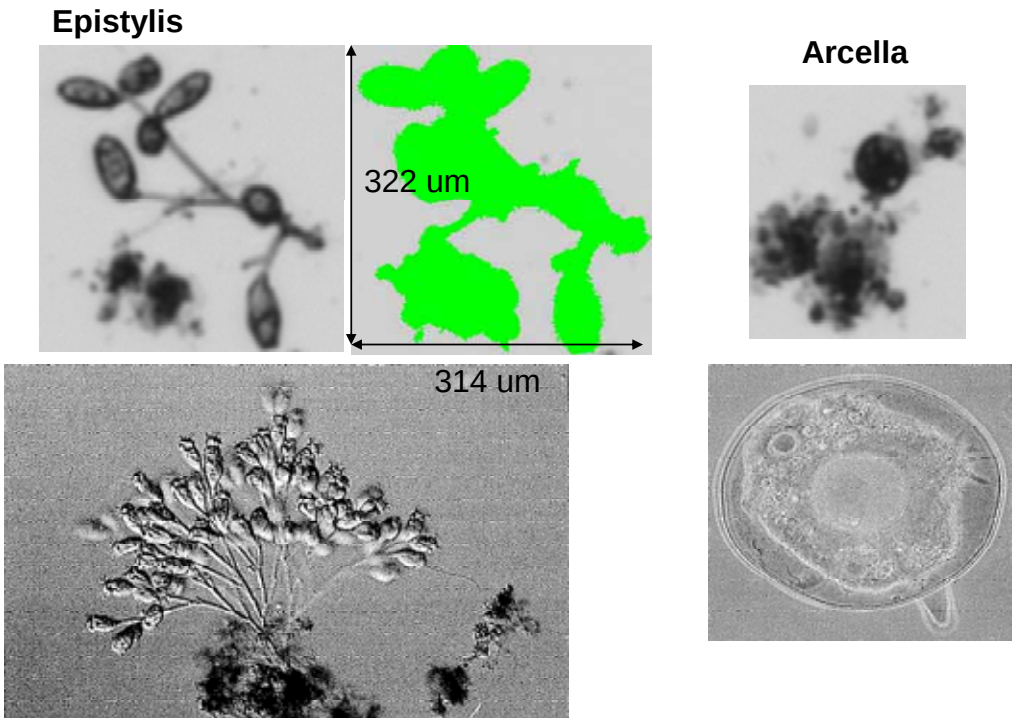

Figure 4.4. Different types of microorganisms seen by image analysis (top images) and light microscopy (bottom images) of Epistylis and Arcella.

On figure 4.4 different microorganisms are observed by the image analysis system, and it can see that the resolution of the pictures is good an image analysis can be used to

identify different microorganisms like epistyles that are common at activated sludge treatment.

The threshold is the process by which the system differentiates between the darker pixels that represent a particle versus the brighter pixels that represents the carried fluid. Figure 4.5 shows how this process occurs. Black shows the particles and white background is the fluid.

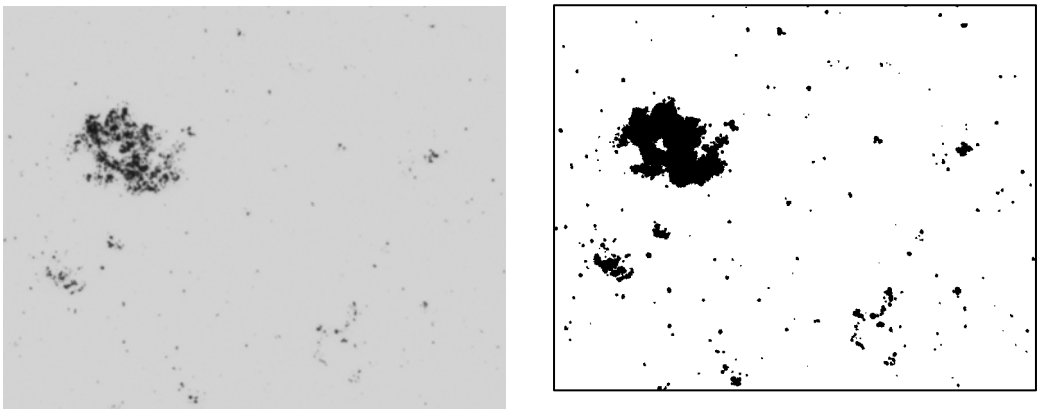

Figure 4.5. Particles separation from the carrier fluid

4.2 Correlation parameters for Latex beads

4.2.1 Correlation tables

Table 4.1 shows selected images of latex beads taken from the image analyzer for average size of 90µm latex beads were introduced to the water in the cell, with its corresponding ECD, area, circularity and feret max diameter. Pictures were taken and the parameters for each particle were calculated.

Number	ECD (µm)	Area (px)	Circularity (0–1)	Feret Diameter Max(µm)	Picture
1	83.13	4511	0.56	88.13	
2	87.38	4919	0.56	91.38	
3	116.13	8057	0.48	163.38	
4	118.63	8381	0.51	162.13	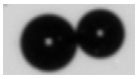
5	151.88	13104	0.51	253.38	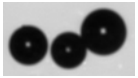
6	175.63	16655	0.45	225.13	
7	185.88	18270	0.45	214.13	
8	198.63	20365	0.4	354.63	
9	180.13	17357	0.24	535.88	
10	226.88	25942	0.2	456.38	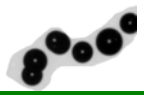

4.2.2 ECD and Circularity relationship

Picture number 1 shows a single circle particle. In this case, the Feret number and the Equivalent Circle Diameter (ECD) are the same, 88.3 μm. This is within the standard deviation of 90 μm for this latex bean. However, the circularity is 0.56, a number that is much lower than in the specifications. This might be a result of the imaging analysis program which takes the bright hole in the middle of the bean, achieving as a hole in the middle of the bean. Thus the circularity becomes lower.

The following pictures show a few particles that are attached one to another. A linear relationship is noticeable between feret diameter and the number of particles that join each other in a row. For example, a feret of 88 μm is obtained for one latex bead particle, 162 μm for two particles in a row, 254 μm for three particles in a row and 355 μm for four particles in a row. When particles join each other in other more compact configurations (not in a line), the feret max is less than that obtained if the same number of particles will be theoretically stretched in a continuous row. It is possible to see that the particles create sedimentation and that the parameters change. The circularity goes down when the particles make a chain. It is possible to see that when particles that are alone like the first and second ones, that the ECD and the Feret number are almost the same, but the circularity is only 0.56. This does not reach the specification of 0.8. When the particles are longer, the circularity is very low and the difference between the ECD and Feret is larger. Particles that aggregate as shown in pictures number 6 and 7, have circularity greater than particles that aggregate in chain, as shown in picture number 8. Using imaging analysis it is possible to analyze defined particles and if enough particles are sampled and relate their characteristics to a statistical data. It is difficult to understand results obtained even for particles that are originally relatively spherical with narrow PSD in their disperse state. However, working with mean diameters can lose information while feret number is not a mean parameter and it relates to the actual raw particle information.

4.3 Particles size distribution for Polystyrene microspheres

Figure 4.6 and Figure 4.7 represents 5 and 10µm polystyrene microspheres which have a normalized particle count of approximately 53 and 45. Two types of polysterene microspheres were analyzed in this study, where an ECD of 5 µm correlated to an average feret diameter of 5.55 µm and an average ECD of 10 µm correlated to and average feret diameter of 10.4 µm. Thus, with disperse spherical particles, the ECD and feret diameters match. In some cases the particles attach to each other as seen in figure 4.7. These are particles that are very close to one another. To understand the floc characteristics, samples that are uniform and spherical were first analyzed.

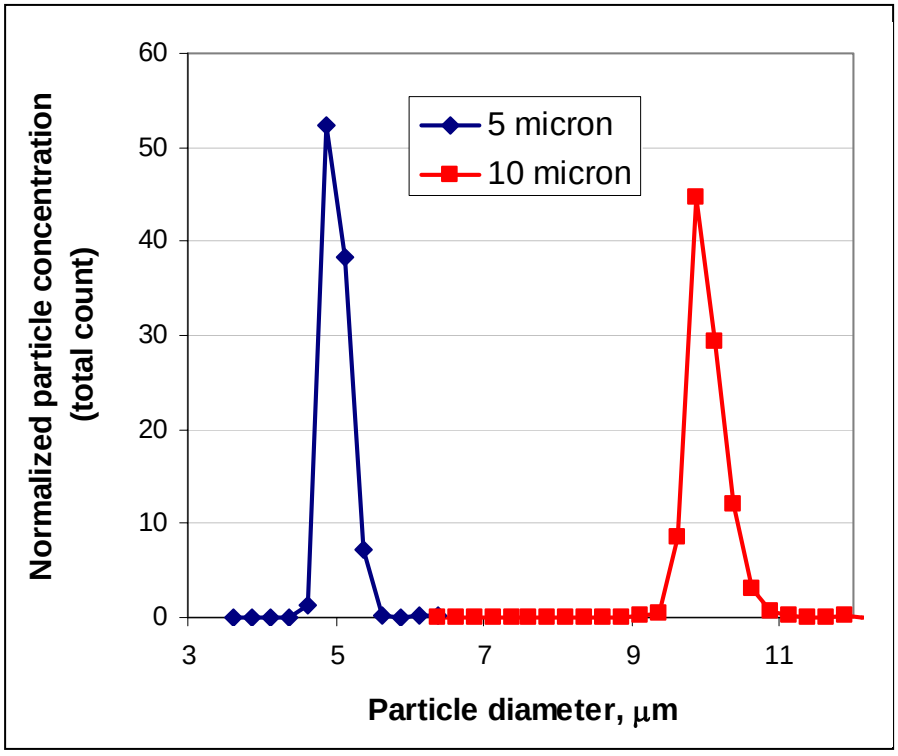

Figure 4.6. Particle size distribution for 5 and 10 µm

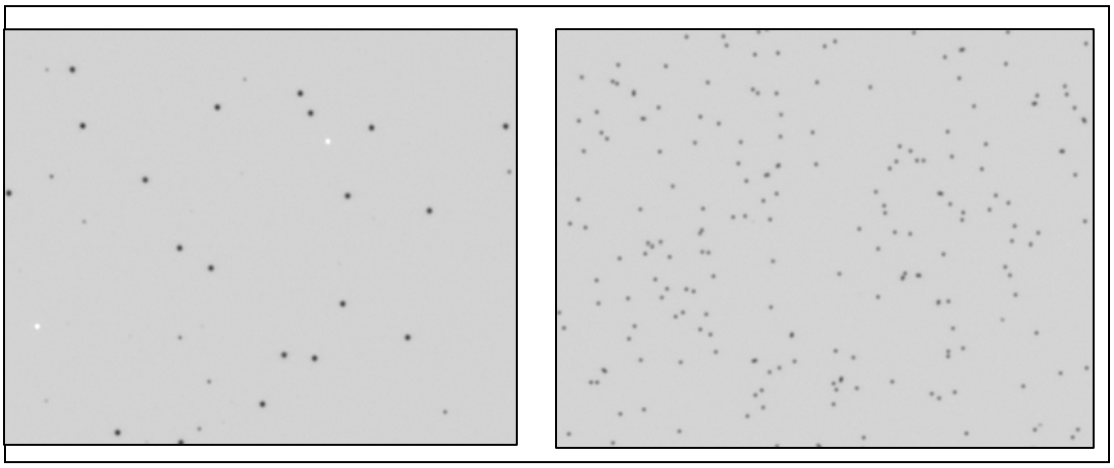

Figure 4.7. Images of 5 and 10μm polystyrene microspheres

4.4 Filtration result

4.4.1 System description

The filter consists of a 0.7 meter top layer of anthracite with a porosity of 0.27 and 0.7 meter lower layer of sand with a porosity of 0.43, and a gravel support layer. The diameter of the filter is 0.609 meter. The filter system is shown in Figure 4.8.

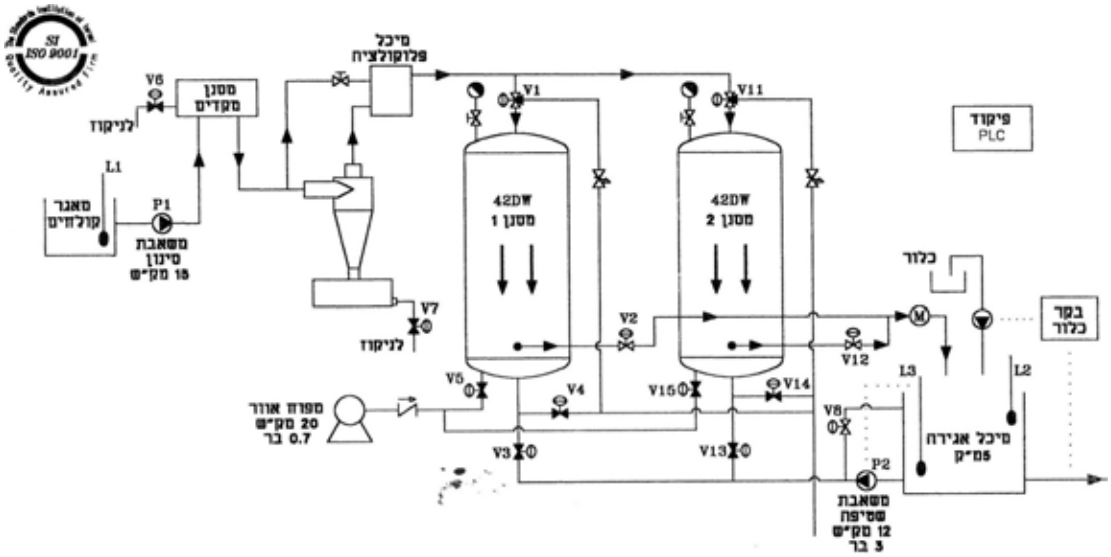

Figure 4.8. Filter system scheme

4.4.2 Retention Time

The retention time of the water in the filter was calculated to represent when the effluent samples that enters the filter gets out. The retention time is calculated for the filter volume, as shown in Figure 4.8 and eq. 4.1. The inlet valve (V1 and V11) is at the top of the filter and closes when the filters start a backwash.

Volume for filter:

$$(4.1)\ \frac{\pi \times d^2}{4} \times L = \frac{\pi \times 0.6096^2}{4} meter^2 \times 0.7 meter = 0.2043 meter^3$$

Effective volume for anthracite: $0.2043 \times 0.27 = 0.05516 meter^3$

Effective volume for sand: $0.2043 \times 0.43 = 0.08785 meter^3$

Filter effective volume: $0.05516 + 0.08785 = 0.14301 m^3$

Retention time for a velocity of 12–13 m/hr when the flow is ~3.6 m^3/hr:

$$\frac{0.140301}{3.6} = 0.0397 hr \longrightarrow 2\text{minutes}\ 22.92\text{seconds}$$

The time that takes to a molecule of water pass through the filter is in average 2 minutes and 23 second.

4.4.3 Suspended solids and turbidity

The filtration process is mostly necessary to reduce turbidity level (NTU) and total suspended solids to achieve Israel Irrigation limits. Wastewater effluent prior to filtration has a turbidity level of 2.5–4.5 NTU and on average is usually 2.5 NTU. After standard filtration it becomes 1.2–1.5 NTU, but with the addition of flocculants the results are 0.5–0.6 NTU.

Table 4.1 describes the parameters of the filtration process in the Dan region wastewater treatment plant (WWTP) in Shafdan.

Table 4.1. Shafdan wastewater treatment filtration process parameters

Type of effluent	**Secondary treated**	**After deep bed filtration**	**Filtration efficiency**
Parameter	Dan Region	Dan Region	Dan Region
Turbidity (NTU)	2–6	0.4–0.8	60%–65%
TSS (mg/l)	4–6	1–3	50%–75%
Uvabs	230	210	9%–8
PSD (2–100 µm)	30,000	2,000	95%
Fecal Coliform (N/100 ml)	10^4	<1000	3–4 logs

Table 4.1 represents the main average parameters that were taken during a period of tests that included hundreds of tests under different conditions such as winter, summer, filtration velocity and different concentrations of flocculants. For turbidity, a parameter widely in use, there is a decrease of approximately 60% on average value from the inlet. This is related to the filter in use with the flocculent type. Efficiency of the filter without a flocculant was on average 40%.

Total Suspended Solids (TSS) during the time of the tests was low, much lower than regulation, before filtering. After filtering, TSS was 50% lower than this value. During tests when the TSS was high, 15–20 mg/l, the efficiency of the filter was higher: 70–80%. No pertinent ultraviolet (UV) absorption data was found.

4.4.4. Head Loss for Filtration Period

Figure4.9 shows the head loss and turbidity for the filter with NPAC and PAC treatment. On the left side of the Y axis is the head loss and on the right Y axis is turbidity in NTU. This graph shows full filtration operation up to 300 cm of head loss or when the filter had been in filtration mode for more than eight hours, followed by backwash mode at these conditions. Filtration operation steps are controlled automatically but can be disabled by user intervention.

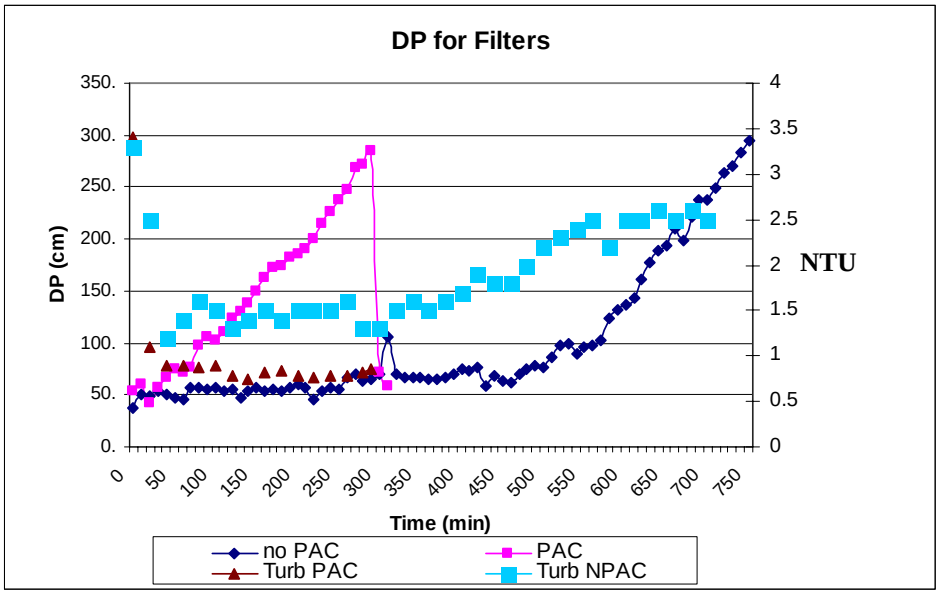

Figure 4.9. Head loss of filter

For this experiment the 8 hour time was disabled therefore the filter continued to run until it reached 300 cm head loss. Filter parameters were observed, head loss is automatically checked by the control panel, and turbidity is measured every 20 minutes. It is seen clearly that the PAC filter has a run time of 5 hours and 20 minutes to reach the backwash time and 13 hours for the NPAC filter. The head loss for NPAC stays constant for 8 hours and after that begins to rise. The turbidity is high for the first 40 minutes of the filter run and remains almost the same for the inflow (between 3.4–3.8 for this experiment). After that, the turbidity remains constant at 1.1–1.8 NTU for the next 7 hours. Breakthrough of the filter follows. This occurs 2 hours after the head loss of the filter begins to rise. In this experiment, when PAC filter reached 300 cm of head loss the filtration run was terminated at that time for both PAC and NPAC filters and backwash followed.

4.4.5. Particle Size Distribution for Filtrate Water

Figure 4.10 shows the particle size distribution that was measured by light scattering for different types of waters, where the higher concentration are for raw water and lower for the filtered water and lowest for filtered water with addition of flocculants . The particles that are smaller than 10 μm have a high concentration and the filtration performance is low. This is applicable to minimum transport mechanism (Adin, 1997).

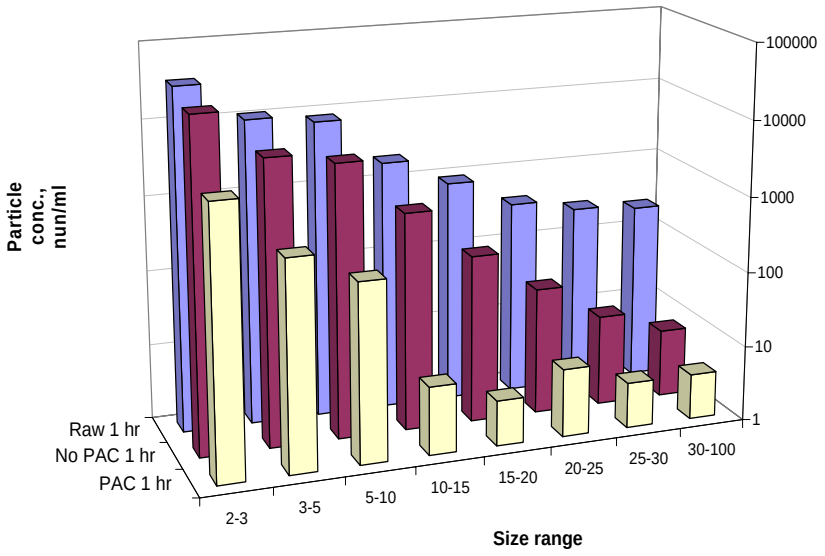

Figure 4.10. Particle size distribution

The problem with light scattering technology is that there is data loss because of the ranges of the particles. When the particle passes through the laser, the result are different that if it is caught from one side to another. This means that the shape affects the result of the test.

4.4.6 Particle Size Distribution at Different Times of Filtration

Figure4.11 represents particle size distribution (PSD) as a function of ECD for water after filtration with or without coagulant treatment. X axis shows the ECD from 2.5–10 micron, while the Y axis represents particle concentration per milliliter of water. The lines represent different times from the start of filtration, beginning with 2.5 minutes, approximately. The time 2.5 minutes was calculated from the retention time for the filter based on the specific porosity of the media water velocity and volume of the media. Therefore 2.5 minutes were subtracted from the actual time effluent samples were taken to obtain a corrected time.

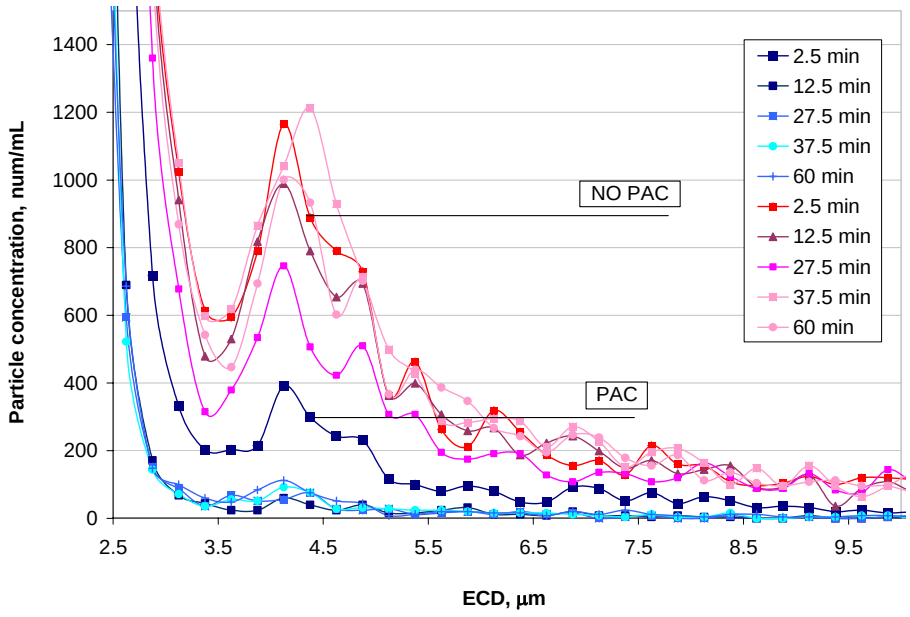

Figure 4.11. Particle size distribution at different times

The blue lines represent PAC treatment, while the red lines represent NPAC treatment. Usually the PSD in wastewater effluents is not normally distributed as observed in this study. According to the PSD and the integrated total count, a higher concentration of particles in the effluent was observed for NPAC filter compared to PAC filter.
Results indicate a large concentration of particles at 2.5–3.5 micron. These are most of the particles present in the water; more than 60%–70% of all the particles in the sample. Particles in water are not normally distributed (Aguilar, 1976) as observed in this study. The higher particle concentration at all ranges of ECD is for the NPAC treatment. Results show that there are more particles compared to the PAC treatment. The larger particles in the inflow raw suspension are probably aggregates of biomass that were not removed in the secondary sedimentation prior to filtration.

Mature time for PAC treatment is 12.5 minutes and particles decreased from 46,000 particles/mL to 5000 particles/mL for 2.5–100 micron and remain lower than 5000 particles/mL during the entire filter run. Small particles (<1μm) are transported by diffusion and can be stopped by the media. Yao et al., (1971) showed that particles 1–2 micron in size are minimally removed from the filter. It is possible that the tendency for the concentration is lower for PAC. In this study, particles less than 2.5 microns were not analyzed therefore there is no data on this type of particle.

Particles that are 3.5 - 5.0 micron in size have a high concentration in PAC and NPAC samples. This may imply minimum transport for particles with a dimension close to minimum transport mechanism (Adin and Elimelech, 1989). Microorganisms of that size can pass over the filter such as *Cryptosporidium* (Amirtharajah,A 1988), thus PSD can be used for performance filtration of this size of particles. Particles larger than 5 micron are transported by gravity or interception. For PAC this means that the concentration is much lower when compared to NPAC treatment. This is possible because the coagulant continues to work inside the filter and particles with lower ECD flocculate and become larger.

4.4.7 Relative Removal Efficiency (RRE)

Percent Relative Removal Efficiency (RRE) is calculated by eq. 4.2 where C_i is influent concentration of raw sample and C_e is concentration at the effluent with PAC (PAC) or without PAC (NPAC).

$$(4.2) \quad \% \, RRE = (\frac{C_i - C_e}{Ci}) \cdot 100$$

Influent particles from secondary treatment may show variability in their concentration and size distribution therefore Ci was sampled simultaneously with Ce to determine removal. Percent RRE of particles as a function of ECD is illustrated in figures 4.12 and 4.13. X axis shows the ECD from 2.5–35 micron, while Y axis represents the percentage of RRE.

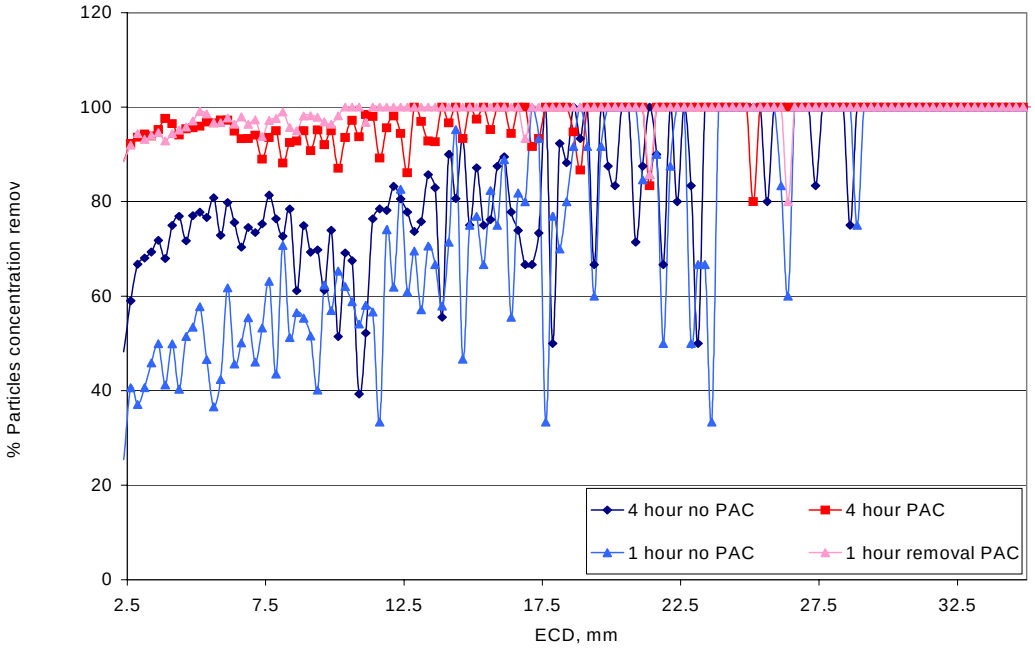

Figure 4.12 Percent RRE of particles as a function of ECD

Figure 4.13 is that same as

Figure 4.12 but shows the removal as per analysis by Adin and Elimelech, 1989.

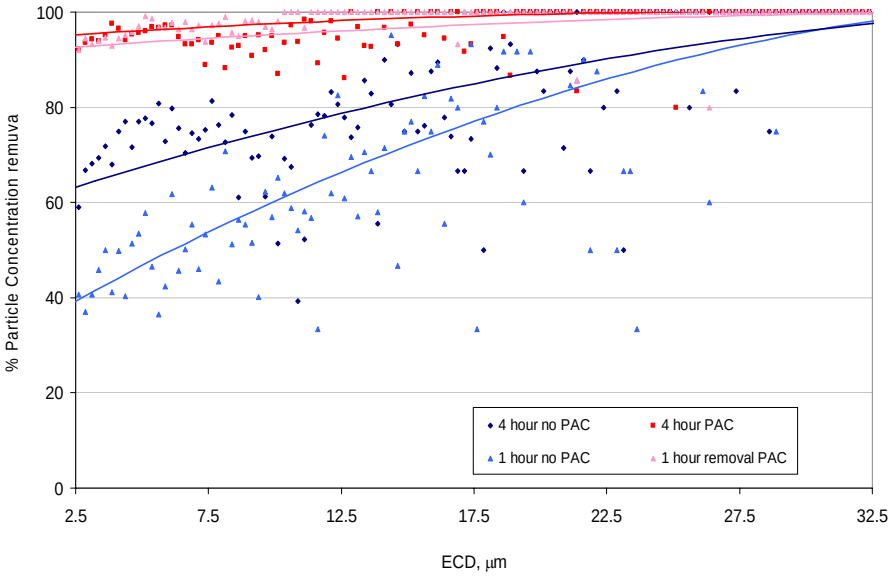

Figure 4.13 Trend for percent RRE of particles as a function of ECD

The samples were taken simultaneously at 1 hour and 4 hours after filtration. Particle count was measured close to the sampling time as possible. The removal processes occurs with the attachment of particles to the filter media or to other particles, large molecules and microorganisms that were attached before (Darby et al., 1992).

The removal of particles is more efficient with PAC treatment than without PAC treatment. It is clearly shown that the use of coagulant improves filter removal efficiency (Stumm and Morgan, 1962). For NPAC, after 1 hour, for particles smaller than 10 micron, removal was low, 40% - 60 % and for large particles removal was improved at 60%–85%. It can be seen that after 4 hours, the RRE improves and is 60%–80% for particles smaller than 10 micron and 80% - 90% for particles larger than 10 micron. For PAC treatment, it can be seen that the RRE is greater than 85% and that there is not much

difference between 1 hour and 4 hour after filtration. This explains that PAC treatment is also useful in catching small particles.

Figure4.12 shows that spikes can be related to sudden lower particle removal especially when the particles with large ECD are compared with particles that enter the filter. This suggests detachment process (Ives, 1966). It can be seen that detachment process occurs more with NPAC treatment. After 60 minutes of filter run there are more spikes than after 240 minutes. After 240 minutes, particles that are detached from the media are caught with an additional collector and can become an additional collector for other particles (Amirtharajah, 1988). The morphology of particles can be important to the detachment process. Hydrodynamic mechanisms for particle transport can change with the shape (Ives, 1982) of the particles. Particles that are not circular or with low circularity, can enter in spin rotation that can help these particles to leave the streaming flow and go to a collector at the filter and be filtrates. The structure of accumulated deposits in the filter is not equally strong, and under the hydrodynamic forces caused by the flow, this structure is partially destroyed. Thus this may disintegrate already fixed flocs (Minst et al., 1967).

4.4.8 Ripening Time by RRE

Figure 4.14 shows the ripening process of the filter with NPAC treatment by showing the RRE. Every line on this graph represents a different time. The samples were taken from filter inflow and outflow. For two samples that were taken at 12.5 minutes and 37.5 minutes, the removal of the particles in the range of 5–7 μm is almost zero and efficiency of the filter is not good. This is called minimum transport (Adin and Elimelech, 1989). At 1 and 4 hours it can be seen that the RRE is higher by more than 50% at 1 hour and more than 80 % at 4 hours. This shows that the ripening time for an NPAC filter increases the efficiency for a long filtration time and not only the first hour of filtration.

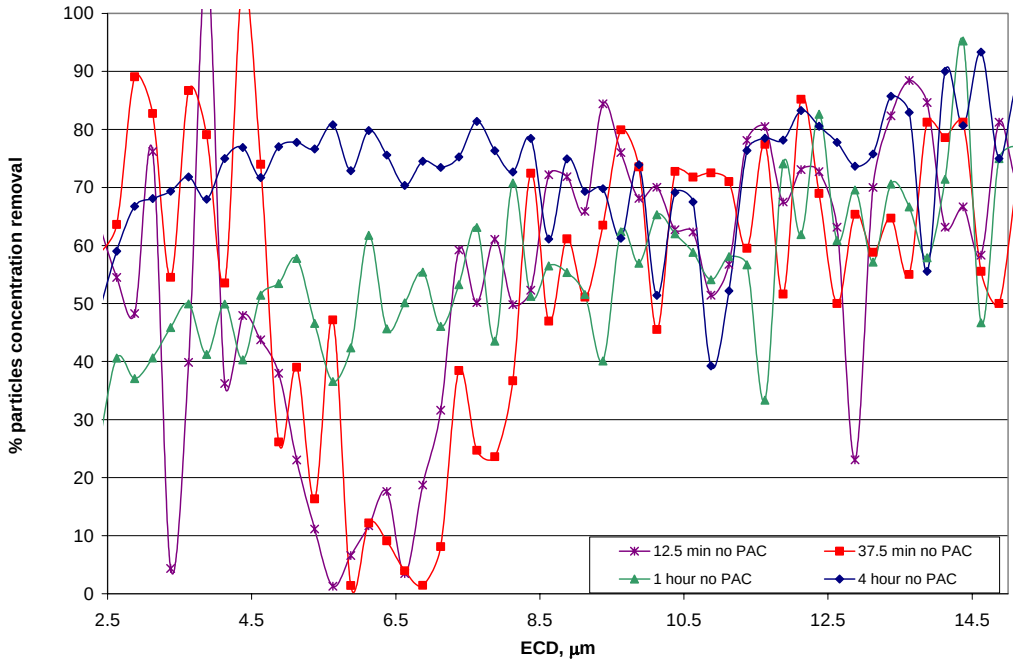

Figure 4.14. Particle size distribution at different times

4.4.9 Particle size distribution comparison for PAC and NPAC samples

Distribution of the particles is similar for influent, PAC and NPAC, but with lower concentrations for PAC sample. It can be seen in Figure4.15 that particles are not normally distributed with concentration above 4 micron for all the water samples.

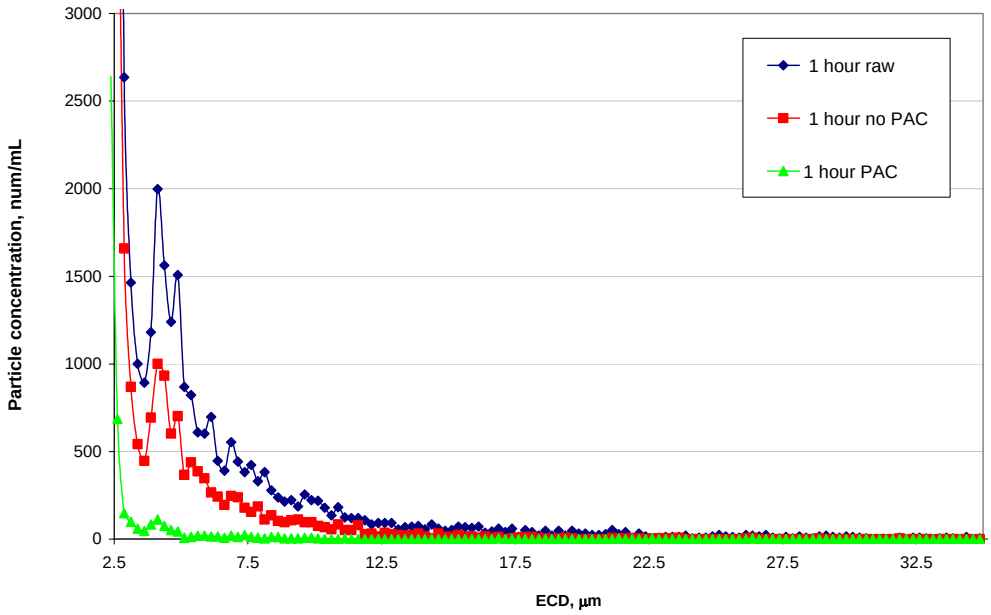

Figure 4.15. Particle size distribution before and after filtration

4.5 Size Distribution for Water after Disinfection

Figure 4.16 shows the samples with chlorine and UV treatment taken from the Ramat HaSharon Wastewater Treatment plant. The samples were held at two reservoirs for 2 weeks after treatment. The sample of chorine was taken to the laboratory and the parameters were determined with imaging analysis.

Figure4.16 shows the ECD versus particle concentration per mL in the wastewater. This is a bimodal distribution with a large concentration of particles from 2.5 µm to 5 µm and a low of concentration particles from 14.4 µm to 18.5 µm. The particles of lower ECD are at a higher concentration.

The wastewater was held at a reservoir for two weeks after chlorine treatment. Possibly algae (chlorophyll was found in the water), reproduced in the water and resulted in bimodal particle distribution at the 14.4 µm to 18.5 µm scale. Particle distribution in water changes with time with natural mechanisms such as flocculation, microorganism

death, reproduction of microorganism, and redox reaction. For these reasons, it is important that the sample is analyzed as soon as possible after sampling time.

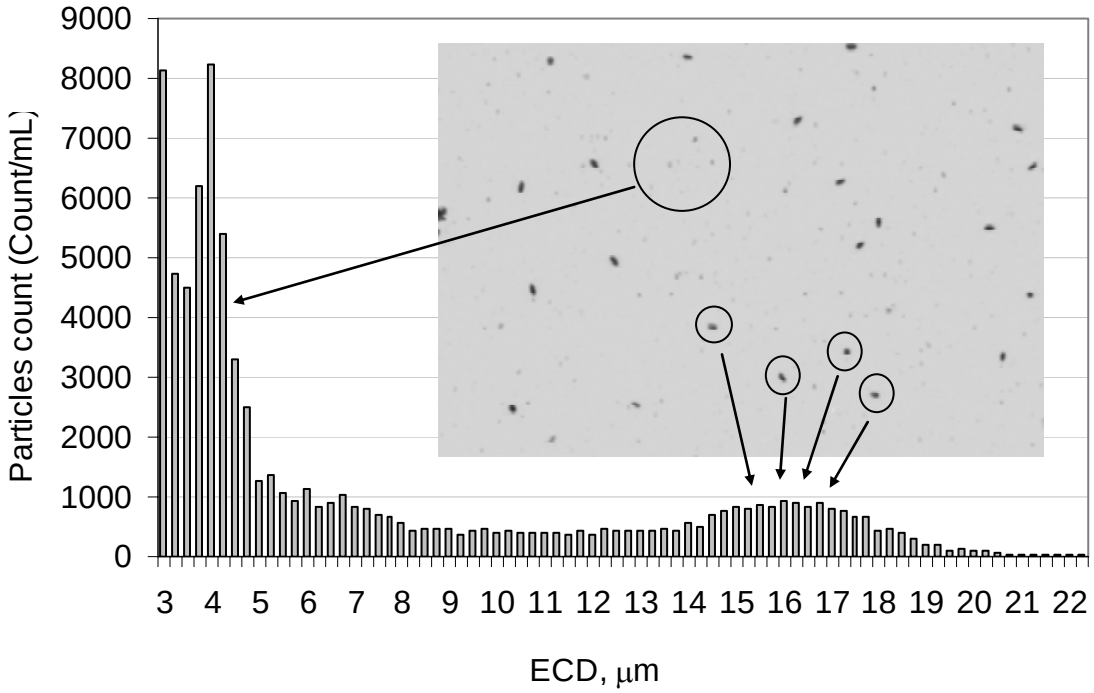

Figure 4.16 Two different particles in large concentration in the same sample

4.6 Relationship between various parameters obtained by image analysis

4.6.1 ECD and Circularity for 90 micron Latex Beads

Figure 4.17 and Figure4.18 show the impact of ECD to circularity with irregular shapes. This experiment was performed with different concentrations of latex beads with average size of 90.7 ±17.7 . The increase of concentration induces the particles to move closer to other particles and results in various particle dimensions. Most of the particles are at approximately 90 microns but there are many particles between the standard deviation of the latex beads, 73–108.4 microns. The low value of circularity at about 0.8 is because two particles attach to each other and form a long particle thus lowering the circularity. The lowest circularity is when the ECD rises and it is obvious that when the particles attach to each other, the circularity is lower.

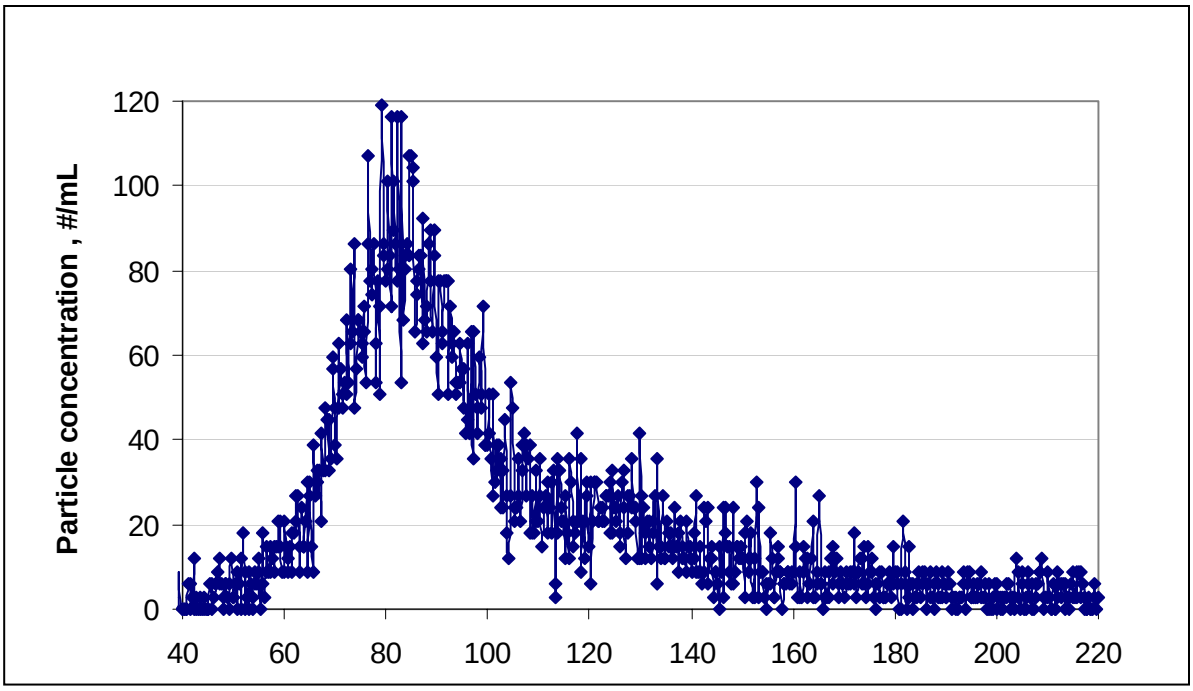

Figure 4.17. Particle size distribution for 90 micron latex beads

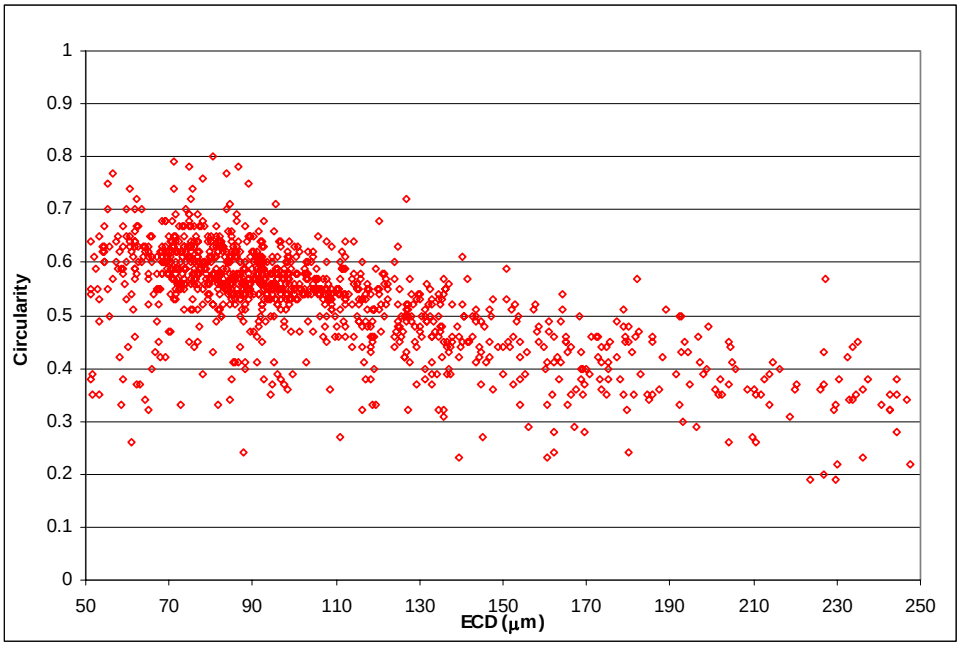

Figure 4.18. ECD as a function of circularity

Figure4.17 and Figure4.18 clearly show the difficulty of interpretation by shape analysis for irregular particles and also for amorphous shape particles.

4.6.2 Circularity vs. ECD for filtrate effluents

Figure 4.19 represents the ECD as a function of the circularity for the influent to the filter, the effluent with PAC treatment, and the effluent without PAC treatment. Figure4.19 represents the sample at 60 minutes after the start of filtration. This graph is built from thousands of particles in each sample in order to check the difference of distribution of the circularity in different characteristic of water.

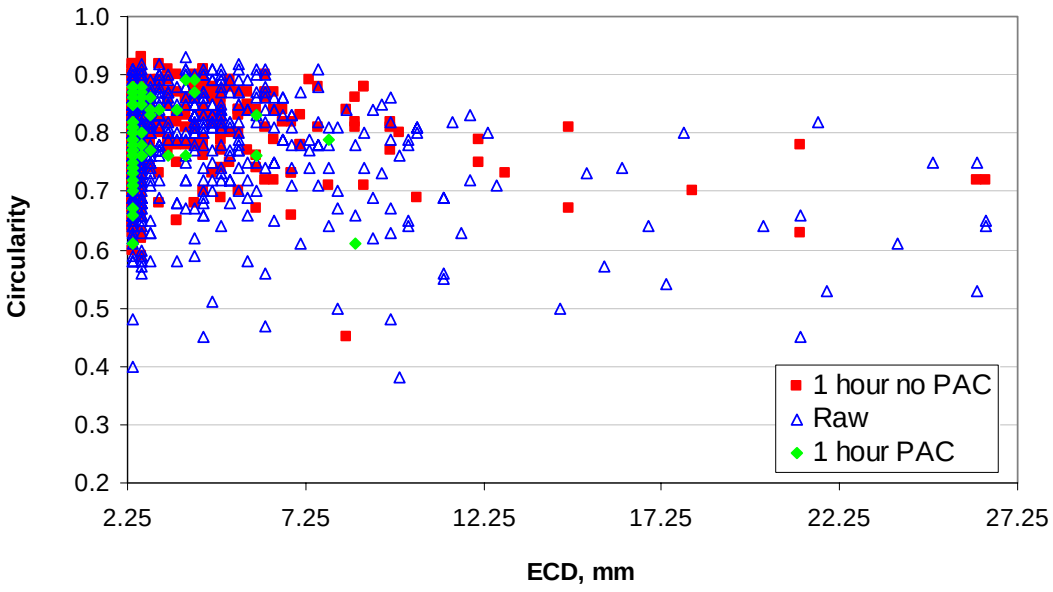

Figure 4.19 Circularity as a function of the ECD for the filter effluent

Figure 4.19 shows that in the PAC treatment the narrow circularity range is between 0.7 and 0.9 and the distribution of the ECD is a maximum of 4 μm for most of the particles. The use of PAC on filtration helps the filter to collect most of the large particles, but also particles than are not round have a greater probability that the PAC will come in contact with the particles and create large flocs that can be collected by the filter media. For NPAC treatment, this shows that the distribution of the circularity is larger between 0.6 and 0.9 and the distribution is a maximum of 30 μm and that NPAC treatment has more

concentration of particles. In terms of the ECD, the larger the circularity of the particles the lower the concentration.

It difficult to come to a conclusion but it can be seen that more particles are larger, that they are not spherical, the circularity of the particles are a maximum of 10 μm, and that particle circularity it not more than 0.8. Another possible reason is that small particles flocculate with themselves and this process is a random process that makes the new particles less spherical than the particles at the start. For raw water it is seen that the distribution for circularity is between 0.4 and 0.9 and the ECD distribution is a maximum 30 μm and has particles that the ECD is it above 100 μm.

4.6.3. Intensity vs. ECD for different particles

Intensity is defined as the sum of all pixel intensities in object divided to the total number of pixels. Particles with higher intensity are more transparent and intensity may provide information about particle makeup. Fig.4.20 shows the intensity of samples as a function of ECD. An inorganic sample taken from soil was separated to the silt fraction was analyzed and termed "Silt", the other particles are as previously determined. Data for the natural particles in the effluent of chlorine, UV and raw filter effluent up to approximately 10 μm fall on top of each other, while the silt particles and the larger mode in the chlorine sample fall on other areas in the graph. Since algae particles can develop in the reservoir of secondary effluents (Adin, 1999), and chlorophyll was detected in both UV and chlorine samples, it is possible that algae particles are dominant in the chlorine samples PSD mode.

Intensity may provide information about particle makeup such as if the particles organic or inorganic. Per the example it can see that the organic fraction of algae between 12 and 18 μm has an intensity from 140–160. For particles that are almost all inorganic, such as the silt sample, it can be seen that the intensity is higher, 165–185., This can mean that organic matter has absorbed the light from the camera and is less transparent.

The optical absorption of inorganic particles such as silt and clay has very high to very low absorbance depending on the elements; organic detritus has generally high

absorbance and biological organisms have usually low absorbance (Rabanski, 2002). The organic detritus particles range from submicron to 100s of microns, while the inorganic particles range up to a few microns. Assuming absorbance is related inversely to particle transparency, may result in higher transparency for biological organisms and lower transparency for organic non-biological matter in effluents.

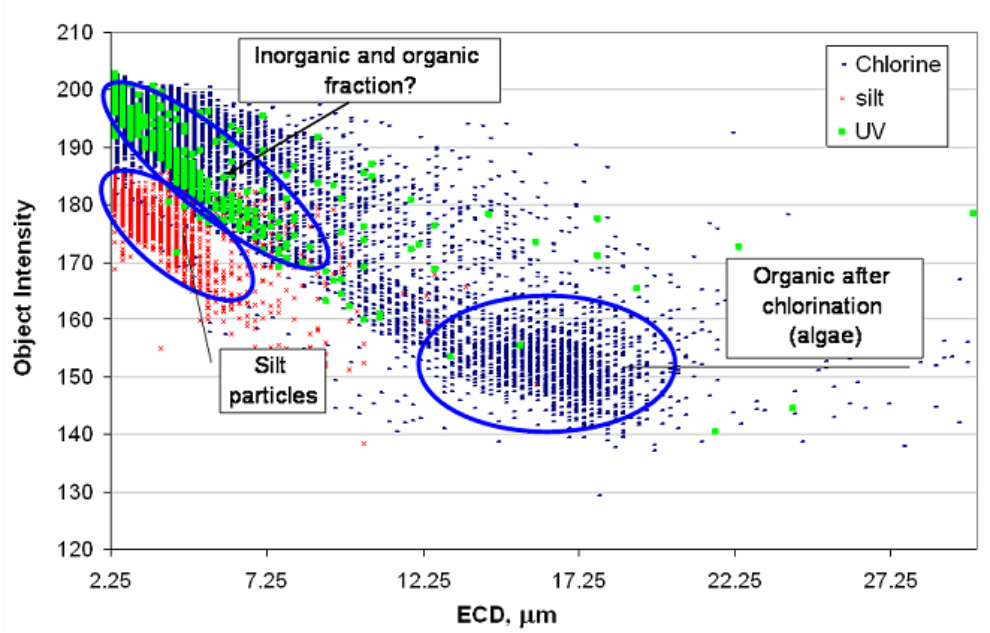

Figure 4.20. Intensity of different particles by ECD

4.6.4. Feret vs. ECD for backwash samples and chlorine reservoir samples

Figure 21 represents the ECD as a function of Feret diameter for backwash water after filtration by PAC treatment and NPAC. The graph represents the data for the two samples that have high concentration of particles, up to 50 µm and shows that particles for the NPAC treatment are mainly 200 µm ECD and 300 µm for Feret. This means there is not much floc and the particles are oval or with irregular shape for particles that came from PAC treatment filtration. A lower count of particles is observed for particles that are larger than 400 µm on ECD and 600 µm on feret, because of the flocculation process

inside the filter and flocs that are captured inside the filter. Feret diameter begins to straighten and when the ECD reaches 900 µm and the Feret 1000 µm, while the ECD continues to be higher and the Feret remains at 1000 µm. This situation may occur because the flocs begin to break when they reach 1000 µm. This means that if the flocs are longer than 1000 µm, the flocs begin to break up and separate into small flocs.

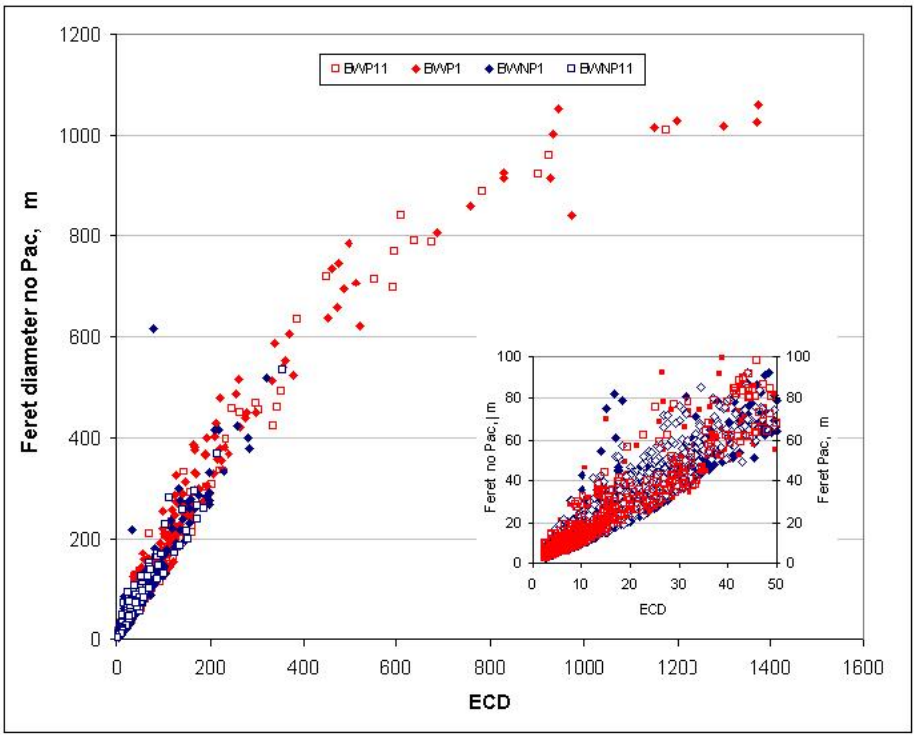

Figure 4.21 Feret vs. ECD for backwash samples

Fig. 4.22 illustrates a 3D plot of ECD as a function of feret number for chlorine sample above. For a particle with a certain ECD, the feret diameter spans over a wide range from circular particles that feret equals to ECD, to elongated particles where feret max is larger than ECD. This data shows that for most particles feret is equal or larger then ECD, thus most of the natural particles in this effluent are elongated even for the small particles. Most of the particles are in the size range up to 3.5 µm, while the small particles are more circular as the feret span in the small particles is narrower compared to larger particles (on ECD basis).

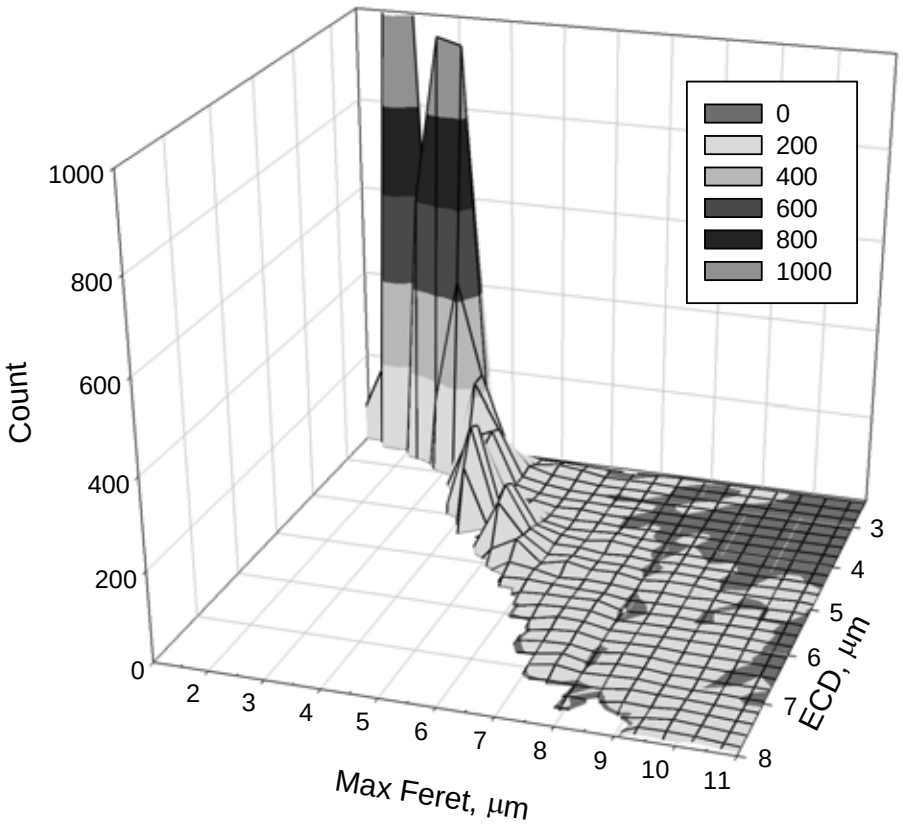

Figure 4.22. 3D plot of ECD as a function of feret max diameter for chlorine samples.

4.6.5. RRE vs. Circularity for PAC and NPAC samples

Figure 4.23 shows the results for RRE vs circularity for PAC and NPC treatment. The differences are significant with the PAC treatment. The RRE is over 80% for all the times and for all circularity. This means that the PAC treatment is useful for catching particles when the circularity is higher. For the NPAC treatment it shows that the filter does not efficiently catch particles when the circularity is higher. Wastewater particle shapes are complex and it seen that the removal for PAC occurs for the entire circularity range except for NPAC treatment. In NPAC treatment, when the circularity is higher, removal is better.

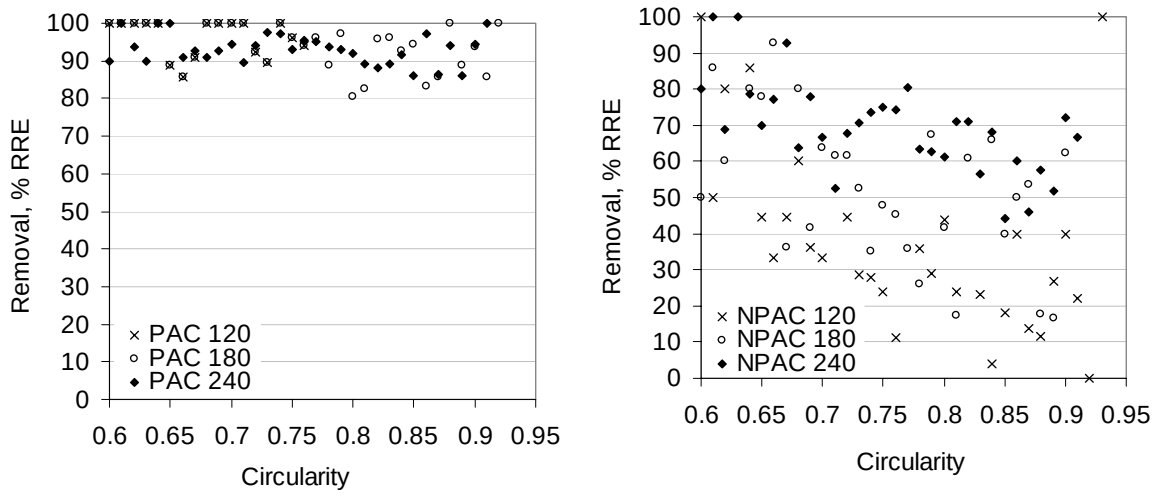

Figure 4.23 Circularity of the particles affecting the RRE

Figure4.24 represents the RRE vs. circularity for particles 2.5–5μm, 5–10μm, and greater than 10μm. RRE is calculated by equation 4.2 . It can be seen that for the entire range of particle size that removal is higher for particle with low circularity. When particles have low circularity, this shape makes to change from the line stream so the particles can be caught by a collector. In the media, it means that the particles have a greater chance of spin thus leaving the streamline and coming closer to the collector at the media. For particles with high circularity, it is seen that the efficiency of the filter is lower and the particles pass throw the filter. For small particles and larger particles, it can be shown that not only is there a detachment process (Minst, 1967) but another process not covered at the literature review. This can be called the streamline process; where particles with the greatest circularity can pass through the media inside the streamline without being collected by the media. In some cases it receives a negative removal based on circularity. This situation only occurs when the particles concentration of the effluent is higher than the influent for the specific circularity. This shows that large particles that have been attached can breakdown into smaller particles. Then the circularity is higher and the particles can enter into the streamline and pass through the filter.

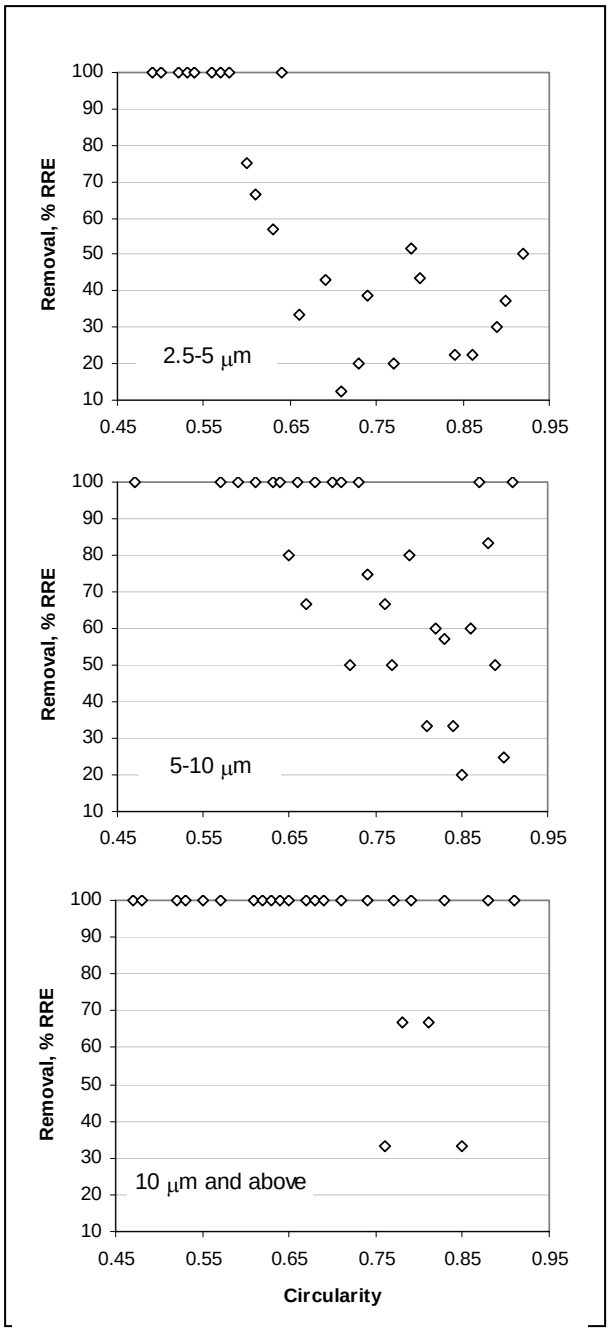

Figure 4.24. RRE basis on the circularity for particles 2.5–5μm, 5–10μm, and greater than 10μm.

It can be seen that particles with circularity greater than 0.65 and in the size range of 2.5–5 μm have less than 50% RRE. This means that the efficiency of the filter is very low for particles with this specific structure. For large size particles the RRE is between 20% and 80%. For particles 5–10 μm and for particles larger than 10 μm, the RRE it almost complete, 100%, with some high parameter than can be because of detachment of particles from the filter. There is no ECD cut off value that will result in complete removal as with a Feret maximum number. For particles that have PAC treatment above a feret of 6–8 μm removal of is 80%–100% but this removal is not found in all samples.

5. Conclusions

1. Filter removal efficiency can be determined by various size and shape parameters, where different information is obtained for each analysis.
2. Results suggest that the particle size distribution is not the sole important characteristics in evaluating water effluents as particles are highly heterogeneous with respect to their size and shape.
3. This method has potential in evaluating efficiency of particle separation processes however more robust statistical analysis need to be used to allow coupling all the size and shape parameters into a meaningful tool to evaluate for example the optimum coagulant dose in contact filtration processes.

References

Adin, A. (1999) Particle characteristics: A key factor in effluent treatment and reuse. Water Res., 40: 67.

Adin, A. and Rebhun, M. (1974).High Rate Contact Flocculation-Filtration with Cationic Polyelectrolyte, *Journal of American Water Works Association*, 66 (2), 109–117.

Adin, A., and Sacks, M. (1991) Dripper clogging factors in wastewater irrigation. J. Irrig. Drain E-ASCE., 117: 813.

Aguilar, M. I., Saez, J., Llorens, M, Soler, A. and Ortuno, J. F. (2003), Microscopic observation of particle reduction in slaughterhouse wastewater by coagulation-flocculation using ferric sulphate as coagulant and different coagulant aids. *Water Res.*, 37, 2233.

Aharoni, A. and Cikurel, H. (2006) Mekorot's research activity in technological improvements for the production of unrestricted irrigation quality effluents. *Desalination.*, 187: 347.

Amirtharajah, A., (1988). Some Theoretical and Conceptual Views of Filtration. *Journal of American Water Works Association*, 80 (6).

Atkinson, J. F. and Cakraborti, R. K. (2006). Dependence of perceived aggregate size pixel resolution using imaging method. *Journal of Water Research and Technology—AQUA*, 55, 7–8.

Chang, Y.., Liu, Q. and Zhang, J. (2005). Flocculation control study based on fractal theory. *J. Zhejiang Univ. SCI,* 6B (10), 1038-–1044.

Churaev, N. V. (1999). The DLVO theory in Russian colloid science., *Adv. Colloid Interface Sci.*, 83,(19).

Clancy, J. L. and McCuin, R. M. (2005). Use of microscopic fluidic imaging for identification and quantification of organisms in water. Am. Water Works Ass., WQTC Conference

Darby, J. L., Attanasio, R. E., and Lawler, D. F. (1992) "Filtration of Heterodisperse Suspensions: Modeling of Particle Removal and Headloss. *Water Research*. 26 (6), 1069–1079.

Elimelech, M., Gregory, J., Jia., and Williams, R. A. (1955). Particle deposition and aggregation.measurement, modeling, and simulation. Butterworth-Heinemann, Oxford.

Emerick, R.W., Loge, F.J., Ginn, T., and Darby, J,L. (2000) Modeling the inactivation of particle-associated coliform bacteria. Water Environ. Res., 72(4), 432-438.

Glasbey, C. A. and Horgan, G. W. (1994). Image Analysis for the Biological Sciences, John Willey and Sons, Chichester.

Gregory, J. (1998) Turbidity and beyond. Filtr. Separat., 35: 63.

Ives, K.J. Fundamentals of filtration. In Proceedings of the 21st European Federation of Chemical Engineering Event Symposium on Water Filtration, Antwerp, Belgium, 1982.

Krumbein, W. C. and Pettijohn F. J. (1938). Manual of Sedimentary. Appleton-Century-Crofts, New York.

Li, D. H., Ganczarczyk, J. J. (1989). Fractal Geometry of Particle Aggregates Generated in Water and Wastewater Treatment Processes. *Environ. Sci. Technol.* 23, 1385–1389.

Li, D. H., Mints, D. M. (1966). Modern Theory of Filtration: Special Subject No. 10, International Water Supply Congress, Barcelona, International Water Supply Association, London.

Mamane, H. and Linden, K.G. (2006) Impact of particle aggregated microbes on UV disinfection. I: Evaluation of spore-clay aggregates and suspended spores, ASCE J Environ. Eng. 132: 596.

O`Melia, C. R. and Stumm, W. (1967). Theory of water filtration, *Journal of American Water Works Association*, 59 (11),1393–1412.

Parker, J.A., and Darby, J.L. (1995) Particle-associated coliform in secondary effluents: shielding from ultraviolet light disinfection. Water Environ. Res., 67: 1065.

Rabanski, G. and King, F. D. (2002). Beyond turbidity— – A quantifiable analysis of solids in drinking water. ICHW.

Sadar, M. J. (1996). Understanding Turbidity Science. Hach Company Technical Information Series, Booklet No. 11.

Stewart, M.H., and Olson, B.H. (1996) Bacterial resistance to potable water disinfectants. Modeling Disease Transmission and Its Prevention by Disinfection, C.J. Hurst, ed. Cambridge University Press, Cambridge, 140-192.

Stumm, W. and Morgan, J. (1962). Chemical Aspect of Coagulation. *AWWA*, 54 (8).

Tufenkji N., Miller G., Ryan, J., Joseph N., Ronald W., Harvey, R. W. and Elimelech, M. (2004). Transport of Crystoporidium Oocysts in porous media: Role of Straining and Physicochemical Filtration. *Environ. Sci. Technol.,* 38, 5932–5938.

Whiple and Jackson (1900). A comparative study of methods used for the measurement of turbidity of water,. *M.I.T. Quarterly*, 13 (274).

Yao, K.., Habibian, M. T., O`melia, C. R. (1971). Water and Wastewater Filtration: Concepts and Applications. *Journal Environmental Science & Technology*., 5 (11), 1105–1112.

APPENDIX A:

Figure A-1 represents a pilot project where all tests were done.

Figure A-1 Overview of pilot plant

The blue tanks are sand filters. The yellow tank is an accumulation device for flocculants and chlorine. The large black tank on the left is an accumulation tank for post-filtration water.

Figure A-2. Overview of sand filter

תכונה זו יכולה לתת הרבה אינפורמציה בסינון חול כאשר חלקיק שהעיגוליות שלו נמוכה יהיה לו יותר קל לסטות מקווי הזרימה ולהיתפס על ידי המסנן, כלומר לחלקיק יש סיכוי יותר גדול להיכנס לסחרור ולצאת מקו הזרימה ולהגיע קרוב למדית המסנן .לחלקיקים בעלי עיגוליות גדולה, נראה שיעילות הסינון קטנה וחלקיקים עוברים את המסנן.

הדמית חלקיקים יכולה לאפיו מיקרואורגניזמים ופלוקים והמידע הזה יכול להיות שימושי בחקר מי השפכים כי נותן את האפשרות לזהות מיקרואורגניזם בשפכים וכך לחקור את שפכים דבר שיכול לעזור בעיקר לתהליכים ביולוגים בשפכים.